The Calabrian Arc subduction complex in the Ionian Sea: Regional architecture, active deformation, and seismic hazard

A. Polonia,[1] L. Torelli,[2] P. Mussoni,[2] L. Gasperini,[1] A. Artoni,[2] and D. Klaeschen[3]

Received 21 October 2010; revised 9 July 2011; accepted 16 August 2011; published 28 October 2011.

[1] We analyzed the structure and evolution of the external Calabrian Arc (CA) subduction complex through an integrated geophysical approach involving multichannel and single-channel seismic data at different scales. Pre-stack depth migrated crustal-scale seismic profiles have been used to reconstruct the overall geometry of the subduction complex, i.e., depth of the basal detachment, geometry and structural style of different tectonic domains, and location and geometry of major faults. High-resolution multichannel seismic (MCS) and sub-bottom CHIRP profiles acquired in key areas during a recent cruise, as well as multibeam data, integrate deep data and constrain the fine structure of the accretionary wedge as well as the activity of individual fault strands. We identified four main morpho-structural domains in the subduction complex: 1) the post-Messinian accretionary wedge; 2) a slope terrace; 3) the pre-Messinian accretionary wedge and 4) the inner plateau. Variation of structural style and seafloor morphology in these domains are related to different tectonic processes, such as frontal accretion, out-of-sequence thrusting, underplating and complex faulting. The CA subduction complex is segmented longitudinally into two different lobes characterized by different structural style, deformation rates and basal detachment depths. They are delimited by a NW/SE deformation zone that accommodates differential movements of the Calabrian and the Peloritan portions of CA and represent a recent phase of plate re-organization in the central Mediterranean. Although shallow thrust-type seismicity along the CA is lacking, we identified active deformation of the shallowest sedimentary units at the wedge front and in the inner portions of the subduction complex. This implies that subduction could be active but aseismic or with a locked fault plane. On the other hand, if underthrusting of the African plate has stopped recently, active shortening may be accommodated through more distributed deformation. Our findings have consequences on seismic hazard, since we identified tectonic structures likely to have caused large earthquakes in the past and to be the source regions for future events.

Citation: Polonia, A., L. Torelli, P. Mussoni, L. Gasperini, A. Artoni, and D. Klaeschen (2011), The Calabrian Arc subduction complex in the Ionian Sea: Regional architecture, active deformation, and seismic hazard, *Tectonics*, *30*, TC5018, doi:10.1029/2010TC002821.

1. Introduction

[2] The CA is part of the most active seismic belt in Italy, and the Ionian Sea has been described as the last remaining segment of oceanic crust subduction in the central Mediterranean [*de Voogd et al.*, 1992; *Faccenna et al.*, 2001, 2004; *D'Agostino et al.*, 2008]. The thick sedimentary section of the African plate, at the toe of the CA (Figure 1), has been scraped off from the descending plate, and piled up along thrust faults resulting in the emplacement of a thick (up to 10 km) and about 200–300 km wide accretionary complex. The regional geometry of the subduction complex has been described from seismic data [*Rossi and Sartori*, 1981; *Finetti*, 1982; *Cernobori et al.*, 1996; *Doglioni et al.*, 1999; *Minelli and Faccenna*, 2010], but the fine-scale structure of the accretionary wedge, i.e., location of the plate boundary, depth of the basal detachment, geometry and structural style, is still poorly constrained. There is little consensus regarding the location and geometry of the major faults absorbing plate motion, as well as the exact position of the outer deformation front of the accretionary wedge. In particular, one major question remains unanswered: is the Calabria subduction zone still active? The lack of seismicity with a characteristic shallow dipping thrust-type focal mechanism along the subduction fault plane can be interpreted in three ways: 1) subduction has ceased [*Wortel and Spakman*, 2000; *Goes et al.*, 2004]; 2) subduction is active but aseismic; 3) subduction is active but with a large locked fault plane

[1]Institute of Marine Sciences, ISMAR-Bo, CNR, Bologna, Italy.
[2]Dipartimento di Scienze della Terra, University of Parma, Parma, Italy.
[3]Leibniz-Institut für Meereswissenschaften (IFM-GEOMAR), Kiel, Germany.

0278-7407/11/2010TC002821

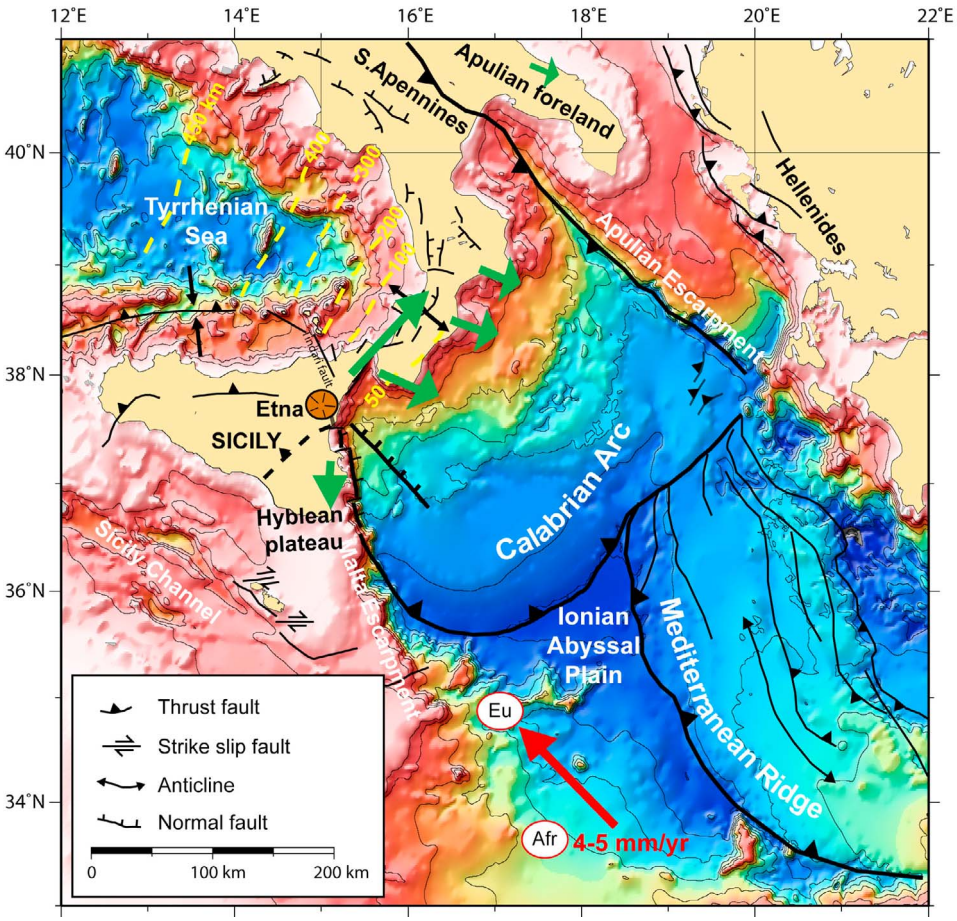

Figure 1. Geodynamic setting of the study area. The geological model is modified from *Morelli et al.* [2004]. Slip vector in the African reference frame is indicated by a red arrow. In green GPS vectors in the Apulian fixed reference frame in which the motion of Calabria is parallel to the slip vector suggesting the existence of active crustal compression as a result of subduction of the Ionian lithosphere beneath the Calabrian Arc [*D'Agostino et al.*, 2008]. The northwest-ward dipping subducting slab of the African plate is represented by the yellow isodepth lines in the Tyrrhenian Sea spacing from 100 to 450 km depth [*Selvaggi and Chiarabba*, 1995]. Eu: Europe, Afr: Africa.

[*Chiarabba et al.*, 2005; *Gutscher et al.*, 2006]. The more external and recently deformed sector of the accretionary wedge, located south of the so-called "external CA" [*Rossi and Sartori*, 1981], shows fold-like structures whose geometry and evolution are driven by shortening and/or salt-tectonic processes due to the presence of Messinian evaporites. Some authors have speculated that the accretionary wedge is presently inactive, and that shortening and large-scale deformation of the wedge could result from passive gravity-driven processes, leading to a collapse of post-Messinian sediments over the evaporites [*Chamot-Rooke et al.*, 2005a]. Others suggest that, despite the slow convergence rate, the CA is the last region in the Central Mediterranean Sea where subduction is still active [*Gutscher et al.*, 2006; *D'Agostino et al.*, 2008]. However, only few studies [*Chamot-Rooke et al.*, 2005a; *Gutscher et al.*, 2006] have focused on the fine structure of the outermost part of the CA system. In fact, high-resolution geophysical data were lacking in this key region of transition between the accretionary wedge and the Ionian abyssal plain.

[3] In the present work we addressed major tectonic issues of the CA, through an integrated approach involving analysis of already available crustal MCS and sparker profiles, multibeam data, and newly acquired high-resolution MCS and CHIRP-sonar profiles in key areas (Figure 2) of the subduction complex. This multiscale integrated approach allowed us to map the fine-scale geometry of the plate boundary, obtain the geological constraints to quantify recent deformation in the outer subduction complex and reconstruct location and geometry of regional active faults absorbing plate motion.

2. Geological Setting

[4] The CA (Figure 1) is part of the eastward migrating Apennine subduction system and connects the NW trending Apennine with the E-W oriented Maghrebian thrust belt [*Patacca and Scandone*, 2004]. It is located above a 300 km wide subduction zone, dipping toward NW characterized by the presence of an active volcanic arc (the Aeolian Islands) and a well defined Wadati-Benioff zone [*Wortel and*

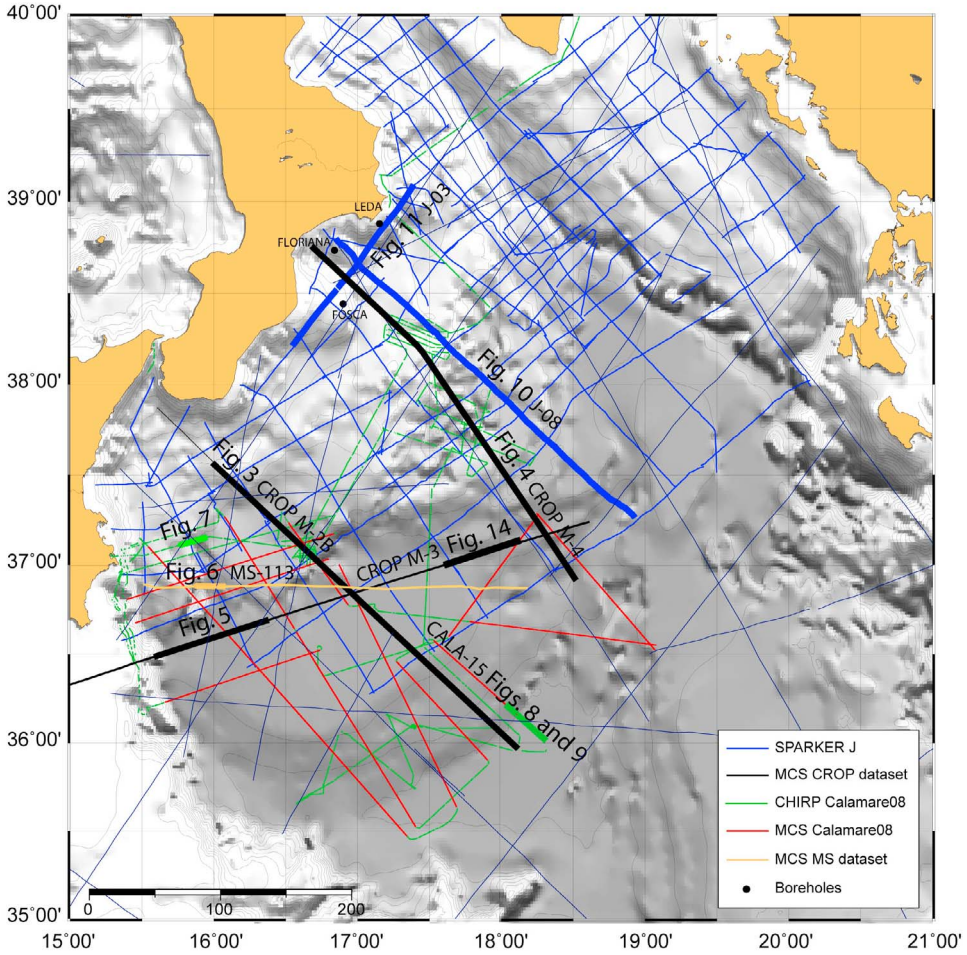

Figure 2. Location of geological and geophysical data available in the working area (morphobathymetry from GEBCO database). Newly acquired data (MCS and CHIRP seismic data) are indicated by red and green lines. Thick lines mark location of seismic profiles described in this work.

Spakman, 2000], with earthquakes descending to nearly 500 km of depth [*Selvaggi and Chiarabba*, 1995]. The Neogene and Quaternary evolution of the CA is controlled by the southeastward retreat of the Apennine-Calabrian subduction zone, that caused rifting and lithospheric thinning culminating in the opening of the Tyrrhenian Sea starting from the upper Miocene [*Malinverno and Ryan*, 1986; *Jolivet and Faccenna*, 2000; *Faccenna et al.*, 2001; *Sartori*, 2003]. Since that time, Calabria has migrated toward SE due to the rapid roll-back of the Ionian-Tyrrhenian slab and trench retreat [*Faccenna et al.*, 2001, 2004]. The high heat flow and the formation of young oceanic lithosphere in the deep Tyrrhenian Sea basins (Vavilov and Marsili) are the result of associated back-arc extension [*Marani and Trua*, 2002; *Zito et al.*, 2003; *Pasquale et al.*, 2005]. Trench retreat was particularly fast over the Neogene and early Quaternary [*Patacca et al.*, 1990] as indicated by high extension rates (50–70 mm/yr) recorded in the Vavilov (Neogene) and Marsili (Early Middle Pleistocene) oceanic seamounts [*Marani and Trua*, 2002; *Mattei et al.*, 2002] and rapid migration of the trench [*Faccenna et al.*, 2001]. On the other hand, vertical axis rotations responsible for the arcuate shape of the CA occurred during Miocene to Quaternary but were almost finished 1 Ma [*Mattei et al.*, 2007] as confirmed by GPS results showing no active back-arc extension in the Southern Tyrrhenian Sea [*D'Agostino et al.*, 2008].

[5] The external part of the arc (Figure 1) is represented by a subduction complex that reaches both the Ionian abyssal plain and the Mediterranean Ridge and is bordered by two major structural features, the Malta escarpment to the southwest and the Apulia escarpment to the northeast. The CA accretionary wedge developed due to the SE-NW Africa/Eurasia convergence, presently occurring at a very slow rate (5 mm/yr or even <5 mm/yr), as reported by recent GPS studies [*Calais et al.*, 2003; *Reilinger et al.*, 2006; *Serpelloni et al.*, 2007; *D'Agostino et al.*, 2008; *Devoti et al.*, 2008]. On the other hand, geodetic investigations of crustal motion in the central Mediterranean have shown significant deviations from the direction of relative motion between the Eurasia and Africa plates [*D'Agostino and Selvaggi*, 2004; *Serpelloni et al.*, 2007; *Devoti et al.*, 2008; *D'Agostino et al.*, 2008]. A significant change in crustal motion occurs between Sicily and the Calabrian Arc [*Pondrelli et al.*, 2004] across the region near the Messina strait [*D'Agostino and Selvaggi*, 2004]. Crustal motion in Southern Sicily is clockwise rotated relative to the predicted motion of Africa and some of the Africa/Eurasia

convergence is probably accommodated offshore northern Sicily [*Hollenstein et al.*, 2003; *Goes et al.*, 2004; *Billi et al.*, 2007] in the southern Tyrrhenian Sea.

[6] Recently, *D'Agostino et al.* [2008], through GPS observations and earthquake slip vectors, suggested that the Adriatic microplate is limited to the South by a newly defined microplate which includes the Apulian promontory, the Ionian Sea and, possibly, the Hyblean region in southern Sicily. This reconstruction describes well the deformation in the Apennines, southern Tyrrhenian Sea and Sicily Channel even though the southern boundary of the newly proposed microplate is not well defined. In this framework the motion of Africa relative to Eurasia is no longer rigidly transferred but rather is accommodated by the opposite rotations of the two proposed microplates (Adria and Apulian/Ionian/Hyblean).

[7] Despite the very slow modern-day plate convergence rates observed by GPS, subduction may still be active in the CA, and subduction rate will depend both on the convergence rate and the velocity of the subduction hinge [*Doglioni et al.*, 2006, 2007]. GPS sites in Calabria (relative to Apulia) show systematic residuals directed toward the Ionian Sea, suggesting active crustal compression and an outward motion of the CA as a result of still active subduction that accounts for the shortening taken up in the accretionary wedge, eventually accommodated by long-term slip on the subduction interface [*Gutscher et al.*, 2006; *D'Agostino et al.*, 2008].

[8] Previous studies have outlined the overall geometry of the subduction complex in the Ionian Sea through the analysis of crustal-scale seismic data [*Finetti*, 1982; *Cernobori et al.*, 1996; *Doglioni et al.*, 1999; *Catalano et al.*, 2001; *Finetti*, 2005], while geological field studies on land have described the inner continental basement rock assemblage made of a nappe pile of metamorphic rocks comprising Tertiary ophiolitic units overlain by a large sheet of pre-alpine continental-derived metamorphic basement with local remnants of Mesozoic-Cenozoic sedimentary cover [*Bonardi et al.*, 2001; *Rossetti et al.*, 2004]. During Oligocene-early Miocene, the metamorphic basement units were affected by crustal extension during Tortonian times [*Mattei et al.*, 2007] while during Pleistocene it experienced high uplift rates, up to 1 mm/yr [*Westaway*, 1993; *Gvirtzman and Nur*, 2001]. These latest tectonic phases affected the inner part of the CA and generated extensional fault systems both parallel and oblique to the coastline [*Del Ben et al.*, 2008]. They are the major tectonic features of the inner portion of the CA that dismember all the older tectonic lineaments.

[9] The submerged portion of the CA consists of a northwestward thickening wedge of deformed sediments [*Finetti*, 1982; *Cernobori et al.*, 1996; *Minelli and Faccenna*, 2010] overlying, in the most external portion, northwestward dipping sediments and the basement. This is structurally consistent with the presence of a SE-verging accretionary wedge [*Cernobori et al.*, 1996]. The wider portion of the slope, named "external CA" [*Rossi and Sartori*, 1981], hosts thrust systems, chaotic units and a province of mud volcanoes [*Praeg et al.*, 2009] that may indicate dewatering of the Calabrian prism due to compressional deformation.

[10] The CA subduction complex is part of the most active seismic belt in the Central Mediterranean region and faces the highly populated regions of Southern Italy, NE Sicily and Calabria that were struck by strong earthquakes in the recent past [*Bottari et al.*, 1989; *Piatanesi and Tinti*, 1998; *Jacques et al.*, 2001; *Galli and Bosi*, 2003; *Gutscher et al.*, 2006; *Jenny et al.*, 2006]. It is therefore vital to unravel the tectonic processes in the submerged portion of the subduction complex that may contribute to seismic and tsunami hazards affecting the region.

3. Crustal-Scale Multichannel Seismic Data Interpretation

[11] We reconstructed the regional architecture of the accretionary complex from MCS data (the CNR_ENI Deep Crust Seismic Profiles - CROP and Mediterranean Sea - MS data sets) acquired during 70s and 90s (Figure 2). We re-processed seismic data at ISMAR-Bo, through a sequence that involves preliminary velocity analysis, Dip Move Out (DMO), velocity analysis after DMO, stack and time migration. CROP seismic profiles were also processed at the Marine Geodynamics Department of the IfM-Geomar (Kiel) within the frame of the EC-IHP (EC-Access to Research Infrastructure) project. We obtained full pre-stack depth-migrated (PSDM) seismic sections, through an iterative migration procedure (the SIRIUS/GXT, Migpack software package), that uses seismic velocities constrained by focusing analysis and common reflection point gathers [*MacKay and Abma*, 1993]. We obtained a very accurate velocity model that includes both lateral and vertical velocity variations in agreement with interpreted geological sections.

3.1. Large-Scale Architecture of the CA Subduction Complex

[12] Western domain: The SE-NW oriented CROP M-2B profile crosses the continental margin from the abyssal plain to the upper continental slope (Figures 2 and 3a) in the western region of the CA subduction system, close to the Messina Strait. The profile is roughly orthogonal to the main structural trends, at least in the outer part of the wedge, providing a seismic image of the geometry of the subduction complex. The continental margin shows an alternation of gentle slopes and terraces that correspond, in depth, to mid-slope sedimentary basins (Figure 3a). The transition from the flat abyssal plain to the gentle topographic slopes that characterize the outermost accretionary wedge is marked by the outer deformation front (s.p. 200). Up to 5.5 km of sediments overlay the African plate basement in the abyssal plain. The incoming sedimentary section can be divided, top to bottom, into 4 main stratigraphic units: a) the 500 m thick and well-layered P-Q unit; b) the Messinian unit, about 1300 m thick and characterized by a transparent seismic facies; c) the Tertiary clastic section (about 1400 m thick) separated from the upper unit by a prominent reflector (B reflector of *Finetti* [1976, 1982]); d) the Mesozoic carbonates (about 2000 m thick) resting on the acoustic basement. Thicknesses and boundaries of these units have been constrained by correlating seismic reflection profiles with seismic refraction analysis [*Makris et al.*, 1986; *de Voogd et al.*, 1992] and published stratigraphic data from the Sirte abyssal plain [*Finetti*, 1976; *Montadert et al.*, 1978; *Polonia et al.*, 2002]. The top of the basement on seismic line M-2B is

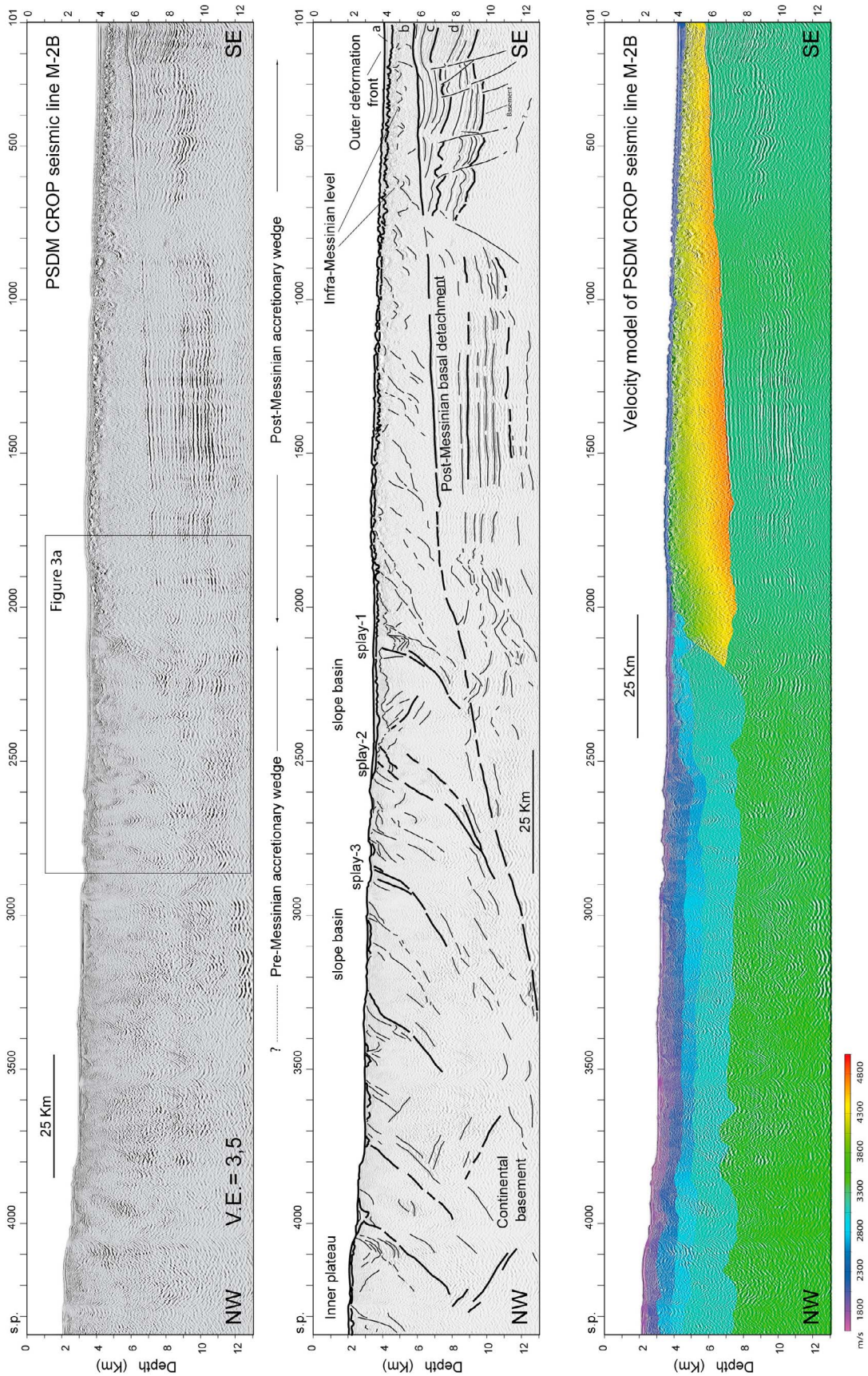

Figure 3a. (top) PSDM (Pre Stack Depth Migrated) MCS line CROP M-2B (see Figure 2 for its location). (middle) Line drawing. (bottom) Color-coded seismic velocities derived from pre-stack seismic data migration. The post-Messinian accretionary complex is clearly evidenced by high seismic velocities (orange and yellow area) at the toe of the continental margin. The salt bearing complex lies above the basal detachment represented by the base of the Messinian evaporites, while the well layered Tertiary and Mesozoic African plate sediments are attached to the lower plate and moves toward NW.

between 9 and 10 km deep, in agreement with seismic refraction data that image the top of what has been interpreted as oceanic crust (reflector 2a of *de Voogd et al.* [1992]) about 9 km below the sea level in the abyssal plain.

[13] The outermost accretionary wedge (s.p. 200–2000) is represented by a salt-bearing complex, with a characteristic acoustically transparent seismic facies, very low surface angle (0.6°) and high seismic velocities, ranging from 4000 to 5000 m/sec (Figure 3a). The basal detachment of the post-Messinian wedge is located along the base of the Messinian evaporites which dips about 0.8° toward NW producing a taper of about 1.5°. From s.p. 200 to s.p. 700 very short wavelength folding affects the top of the Messinian evaporites resulting in an hummocky seafloor morphology that has been termed "cobblestone topography" [*Hersey*, 1965; *Kastens*, 1981; *Kastens and Cita*, 1981; *Rossi and Sartori*, 1981] and interpreted as due to collapse structures driven by karst processes [*Hinz*, 1972; *Ryan et al.*, 1973] or by a combined effect of tectonics and salt diapirism [*Kastens*, 1981; *Camerlenghi and Cita*, 1987]. On the other hand, low-amplitude and very short wavelength folding observed in the outermost part of the wedge may suggest a secondary shallower décollement possibly constituted by an infra-Messinian level (Figure 3a). As for the Mediterranean Ridge, the Messinian lower evaporites act as the main detachment level while the upper evaporites may operate as a disharmonic layer below thin Plio-Quaternary sediments [*Chaumillon et al.*, 1996].

[14] In the abyssal plain and in the outermost wedge seaward of s.p.1000, the Tertiary and Mesozoic sedimentary sequences show evidence of faulting and folding. Sediment deformation is related to thrust faults that reactivate pre-existing normal fault planes bounding rotated blocks. These blocks are delimited by steep landward dipping reflectors that displace pre-Messinian seismic units and slightly deform the base of the Messinian unit. These tectonic features are well imaged in the Prismed data set [*Chamot Rooke et al.*, 2005b] as well as in seismic line MS-27 [*Finetti*, 1982] where the deformation clearly involved growth deposits of Tortonian age. This suggests it probably developed during Tortonian and Serravallian times as proposed by *Chamot-Rooke et al.* [2005b]. During this tectonic phase this segment of the incoming plate was far from the outer deformation front; thus this deformation may not be related to subduction processes but rather to a contractional tectonic phase affecting the African plate margins during Serravallian/Tortonian and Messinian times.

[15] In seismic line CROP M-2B (Figure 3a), at s.p. 700 and 1050 we observe two major sub-vertical deformation zones in the Tertiary and Mesozoic sequences over which layering of the sediments terminates abruptly. We interpret these discontinuities as major tectonic features marking the boundary between two different tectonic and paleogeographic Mesozoic domains. The structures may have been active throughout the Plio-Quaternary, as the upper unit shows abrupt thickness variations along vertical structures (Figure 3a).

[16] The most recent accretionary wedge is bounded toward the NW by a slope terrace that is the seafloor expression of a sedimentary basin showing a rather flat morphology and some depocenters separated by structural highs (Figures 3a and 3b, s.p. 1900–2450). This basin develops above a region where the basal detachment and deeper reflectors abruptly change their dip from 0.8° to the SE to 3.5° to the NW. PSDM seismic velocities confirm that Messinian evaporites are present seaward and below this basin, while landward the wedge is made of rocks characterized by slower seismic velocities (in the range of 2500–3000 m/s) that we interpret as pre-Messinian clastic sediments. This might indicate that the sedimentary thrust top basin formed during Messinian times. The observed transition from evaporitic to clastic assemblages is reflected by the different structural architecture of the innermost wedge, that shows a series of 5 topographic scarps (Figure 3a, s.p. 2400, 2850, 3200, 3800, 4000) separated by sedimentary basins and mid-slope terraces. The scarps are controlled at depth by a series of high angle landward dipping reflectors that we interpret as out of sequence thrust faults (sometimes also referred to as "splay" faults). The out of sequence thrust faults affecting the thrust top basin at s.p. 2450 and 2100 (Figure 3b) are located at the transition between the salt-bearing complex to the SE, and the clastic pre-Messinian wedge to the NW. These faults reflect the structural contrast between a shallow décollement (Messinian evaporites) in the frontal wedge, and a deeper basal detachment within the pre-Messinian sediments, due primarily to differences in rheology, as shown by velocity changes in the PSDM velocity model (Figure 3a). In Figure 3b, we compare the PSDM seismic section across the thrust top basin with the *time migrated* (center) and the *stacked* (bottom) sections, to underline that the out of sequence thrust faults at the rear of the Messininan accretionary wedge are not artifacts related to lateral velocity changes along these features in the PSDM velocity model, but indeed produced by real seismic discontinuities.

[17] At the rear of the wedge, the subduction system is bounded by a seaward dipping reflector representing the top of the continental basement that intercepts the basal detachment at s.p. 3500. Above the continental basement a rather flat and relatively less deformed domain (Inner Plateau) is present.

[18] Eastern domain: CROP MCS seismic line M-4 (Figure 4) has been acquired in the region offshore Calabria orthogonal to the main structural trends (Figure 2). Unfortunately, this line does not reach the outer deformation front as its acquisition has been stopped in a region still belonging

Figure 3b. Close-up view of MCS line CROP M-2B across the slope terrace (see Figures 2 and 3a for location). (top) Pre-stack depth migrated 36 fold MCS line CROP M-2B across the slope terrace at the transition between the post-Messinian salt bearing complex and pre-Messinian wedge. The basal detachment cuts through deeper layers as s.p. 2000 is approached; two out-of-sequence (splay) faults develop to accommodate differences in rheology between the two wedges and basal detachment depth variation. (middle) Time migrated seismic section where landward dipping thrust faults are clearly imaged below the sedimentary basin; this implies that splay faults are not artifacts related to lateral variations in the velocity model used for pre-stack depth migration. (bottom) Stacked section; splay faults are masked by multiple diffractions.

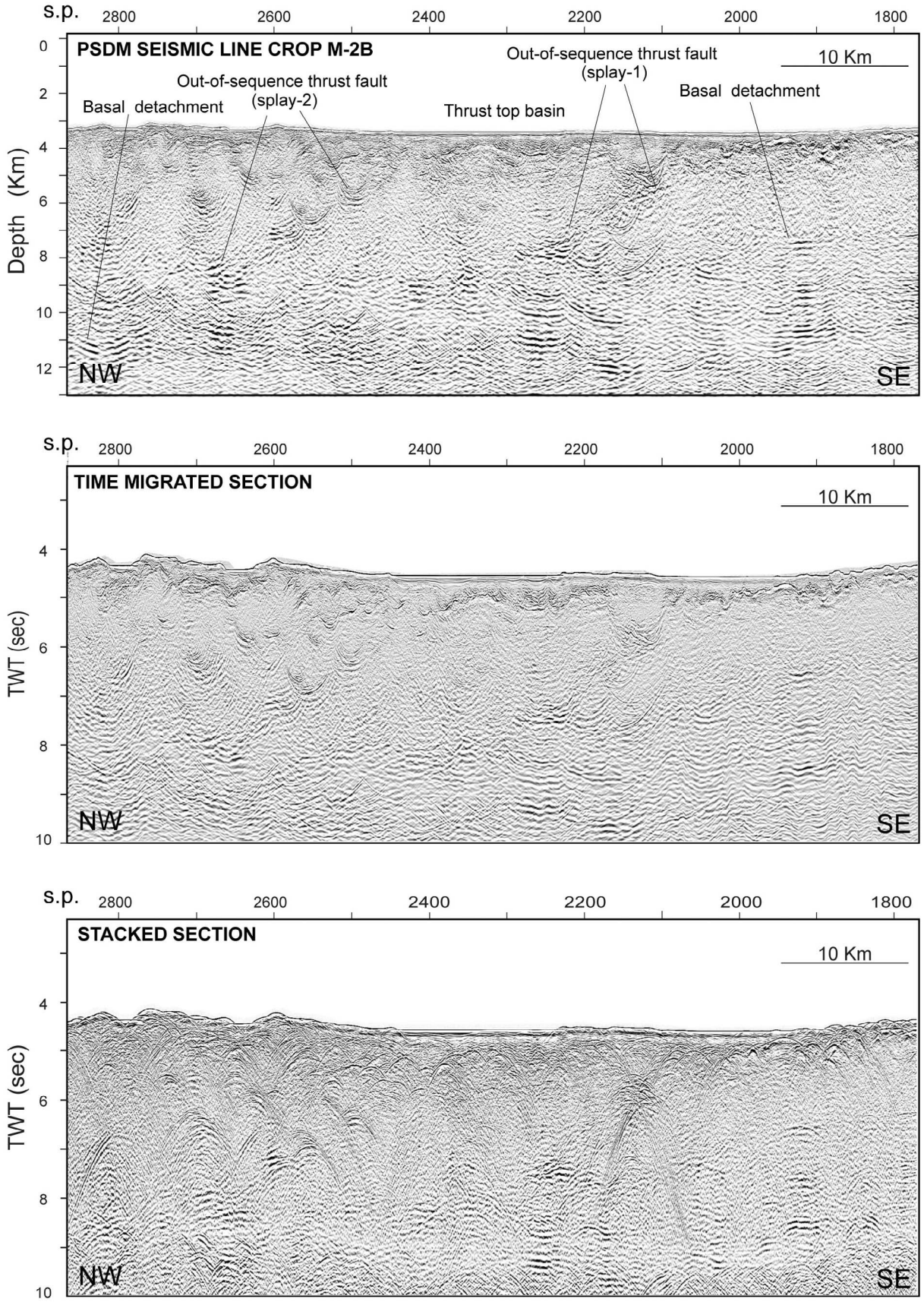
s.p.
2800
2600
2400
2200
2000
1800
PSDM SEISMIC LINE CROP M-2B
10 Km
Out-of-sequence thrust fault (splay-1)
Out-of-sequence thrust fault (splay-2)
Basal detachment
Thrust top basin
Basal detachment
Depth (Km)
0
2
4
6
8
10
12
NW
SE
s.p.
2800
2600
2400
2200
2000
1800
TIME MIGRATED SECTION
10 Km
TWT (sec)
4
6
8
10
NW
SE
s.p.
2800
2600
2400
2200
2000
1800
STACKED SECTION
10 Km
TWT (sec)
4
6
8
10
NW
SE

Figure 3b

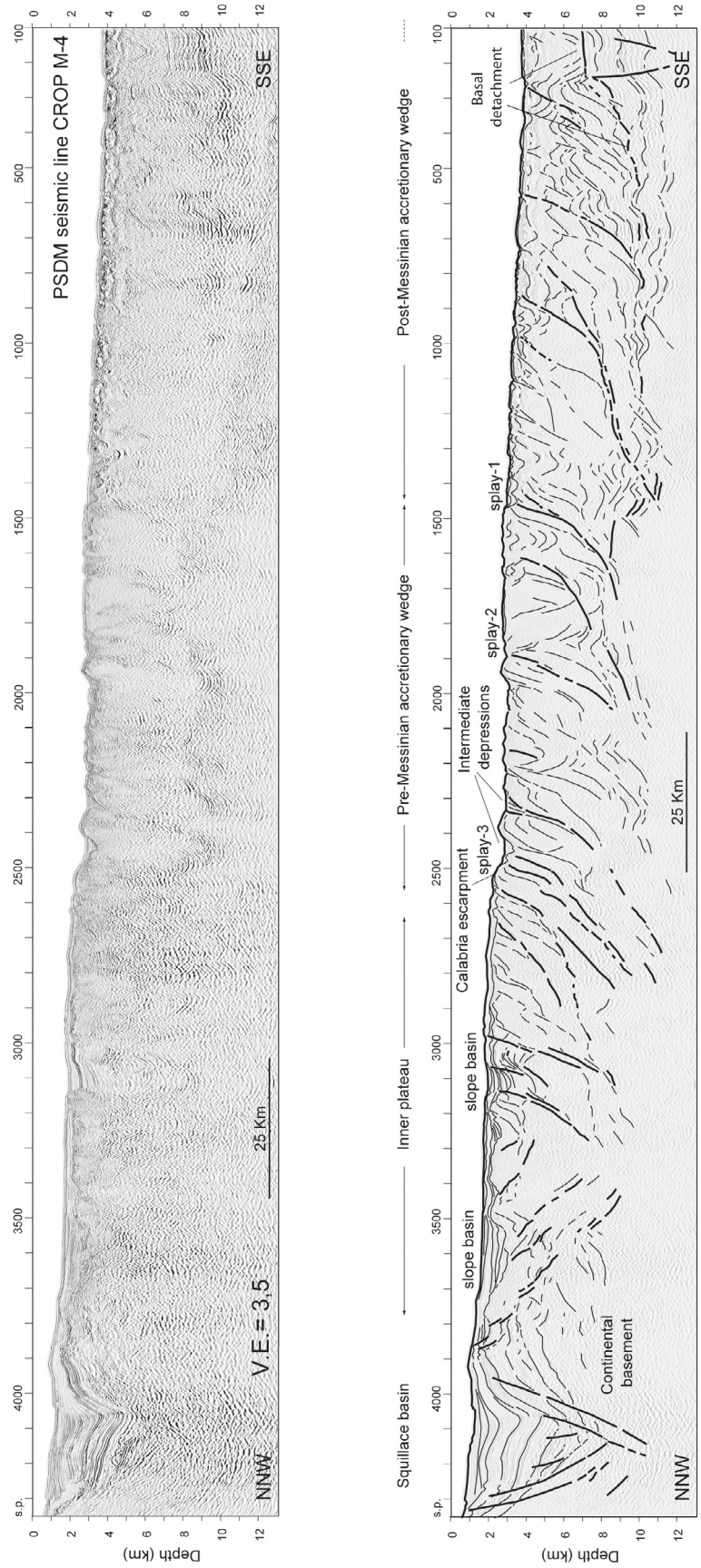

Figure 4. (top) Pre-stack depth migrated 36 fold MCS line CROP M-4 and (bottom) its line-drawing. Location of seismic profile is shown in Figure 2. This profile has been collected in the eastern region of the Calabrian Arc subduction complex. Deformation is related to the presence of duplex structures and an imbricate fan develops to accommodate basal detachment depth variations occurring within the post-Messinian accretionary wedge. Structural style and basement involved tectonics suggest that this region is characterized by higher shortening and uplift rates.

to the outer accretionary wedge. Despite this major limit, this is a key profile to unravel structural style variations in the CA subduction complex. Pre-stack depth migrated CROP-M4 seismic profile, in fact, images a completely different structure of the accretionary wedge relative to the western region described above. To the SSE (from s.p. 100 to s.p. 240), the basal detachment is located at the base of the evaporites while it abruptly deepens at s.p. 240 where a succession of duplex structures and an imbricate fan develop to accommodate basal detachment depth variation. Thrust faults between duplexes control small-scale basin formation at the seafloor and displacements of the upper reflectors suggesting recent tectonic activity. From s.p. 240 to s.p. 800 the detachment cuts through progressively deeper levels down to the basement below the Mesozoic succession and progressively thicker sediment packages are involved in deformation. In this region, despite the presence of evaporites, deformation affects the whole sedimentary section, including the Tertiary and Mesozoic units, and higher shortening and uplift rates are expected. The extent of the salt bearing post-Messinian accretionary wedge can be deduced by the presence of a prominent, high amplitude, but not continuous, reflector at the base of the Plio-Quaternary sediments (top of Messinian evaporites), which is interpreted as related to fluid migration and the presence of free gas. The same reflector and seismic facies at the top of the Messinian evaporites is visible in the profile CROP M-2B (Figure 3a).

[19] The post-Messinian accretionary wedge is bounded toward NNW by a landward dipping thrust fault (splay-1), which produces a scarp along which the seafloor is uplifted of about 250 m. This structural feature represents the transition between the salt-bearing complex to the South, and the pre-Messinian, well layered and highly deformed clastic wedge made of Tertiary and possibly Mesozoic deposits, to the North. Major thrust faults have been correlated to those described in the Eastern domain and named splay-1, -2 and -3.

[20] Splay-3, in particular is marked by a major topographic scarp ("Calabria Escarpment") with about 600–700 m offset, bounding two different tectonic domains. To the South of the Calabria Escarpment, the seafloor is characterized by a very rough topography related to high amplitude and large wavelength folds that produce km-scale sedimentary basins (intermediate depressions of *Rossi and Sartori* [1981]). This region appears to be depressed relative to North and South bounding blocks. Landward of the Calabria Escarpment, a less deformed and rather flat terrace is present (Inner plateau). Here, seaward and landward dipping normal faults contribute to the development of multiple slope basins separated by structural highs. The Inner plateau is bounded toward NNW by the Squillace forearc basin that is a NNW-SSE trending (Figures 1 and 2) forearc basin filled by a 5 km thick sedimentary section.

3.2. The Western Lateral Boundary of the CA at the Toe of the Malta Escarpment

[21] The CA subduction complex is bounded to the W by the Malta escarpment, a major regional NNW-SSE trending morphological feature linking the Ionian basin to the Hyblean plateau, a continental forebulge formed in front of an orogenic recess along the highly irregular African-Eurasian plate boundary [*Billi et al.*, 2006]. The Malta escarpment has been described as a right lateral active transtensional system [*Doglioni et al.*, 2001] re-using a pre-existing Mesozoic continent-ocean transition between Sicily and the Ionian deep basin [*Catalano et al.*, 2001]. *Argnani and Bonazzi* [2005], on the other hand, suggest that only the portion of the Malta escarpment N of Siracusa is characterized by active extensional faults. The oceanic/continental lithosphere transition may occur close to the Malta escarpment [*Chamot-Rooke et al.*, 2005a] but relationships between the CA accretionary wedge and the Malta escarpment are still poorly constrained.

[22] In order to better define nature and activity of this regional boundary, we reprocessed CROP M-3 seismic profile (Figure 2) that crosses along-strike the subduction complex and the Malta escarpment. Figure 5a shows the westernmost part of this profile, where the contact between the Malta escarpment and the accretionary wedge is imaged. At the toe of the escarpment, the lower continental slope appears to be disrupted along at least two East-dipping normal faults that produce two steep scarps of about 700 and 1000 m. At the base of the slope, the seafloor is rather flat because a thick section of Plio-Quaternary sediments completely buries the pre-existing morphology. A more transparent, wedge-shaped unit, progressively thickening toward the East, can be seen below the Plio-Quaternary sequence. It represents the post-Messinian accretionary wedge emplaced above the basal detachment level marked by a prominent reflector at about 6 km depth. This reflector represents the base of the Messinian evaporites, as confirmed by the relatively high migration velocities ranging from 4000 to 5000 m/sec, and the acoustically transparent seismic facies above. The layered seismic units below this level represent the Tertiary clastic and Mesozoic carbonate sediments (Figure 5a). The unit at the base of the post-Messianian accretionary wedge may represent the Tortonian deposits described by *Chamot-Rooke et al.* [2005b] in the area. At the toe of the lower slope, a 700–800 m thick chaotic body is visible, sandwiched between the salt-bearing accretionary wedge and the Plio-Quaternary turbidite units (Figure 5a). We interpret this feature as due to large-scale slumping related to a catastrophic event that occurred in post-Messinian times. It might have been triggered by tectonic processes and/or by volcanic activity (possibly the Mt. Etna) or it may be related to the mid Pliocene tectonic re-organization that has triggered the release of overpressured fluids from within the accretionary wedge with the formation of mud chambers and the inception of mud extrusion processes [*Praeg et al.*, 2009] and slope instability.

[23] About 70 km east of the toe of the Malta escarpment, a lithospheric sub-vertical fault system and a listric fault outcropping at the seafloor offset the accretionary wedge as well as deeper reflectors, and controls the formation of a fan-shaped basin, whose geometry suggests syn-tectonic sedimentation above an East dipping transtensive fault (Figure 5a). The geometry of the sedimentary basin and the displacement of the seafloor (Figure 5b) suggest this fault is presently active, as confirmed by a MCS line MS-113 acquired North of M-3 (Figure 6) showing deformation reaching the seafloor. Fault activity has been investigated from CHIRP data (Figure 7) where two submarine canyons and topographic scarps are present along the fault strands.

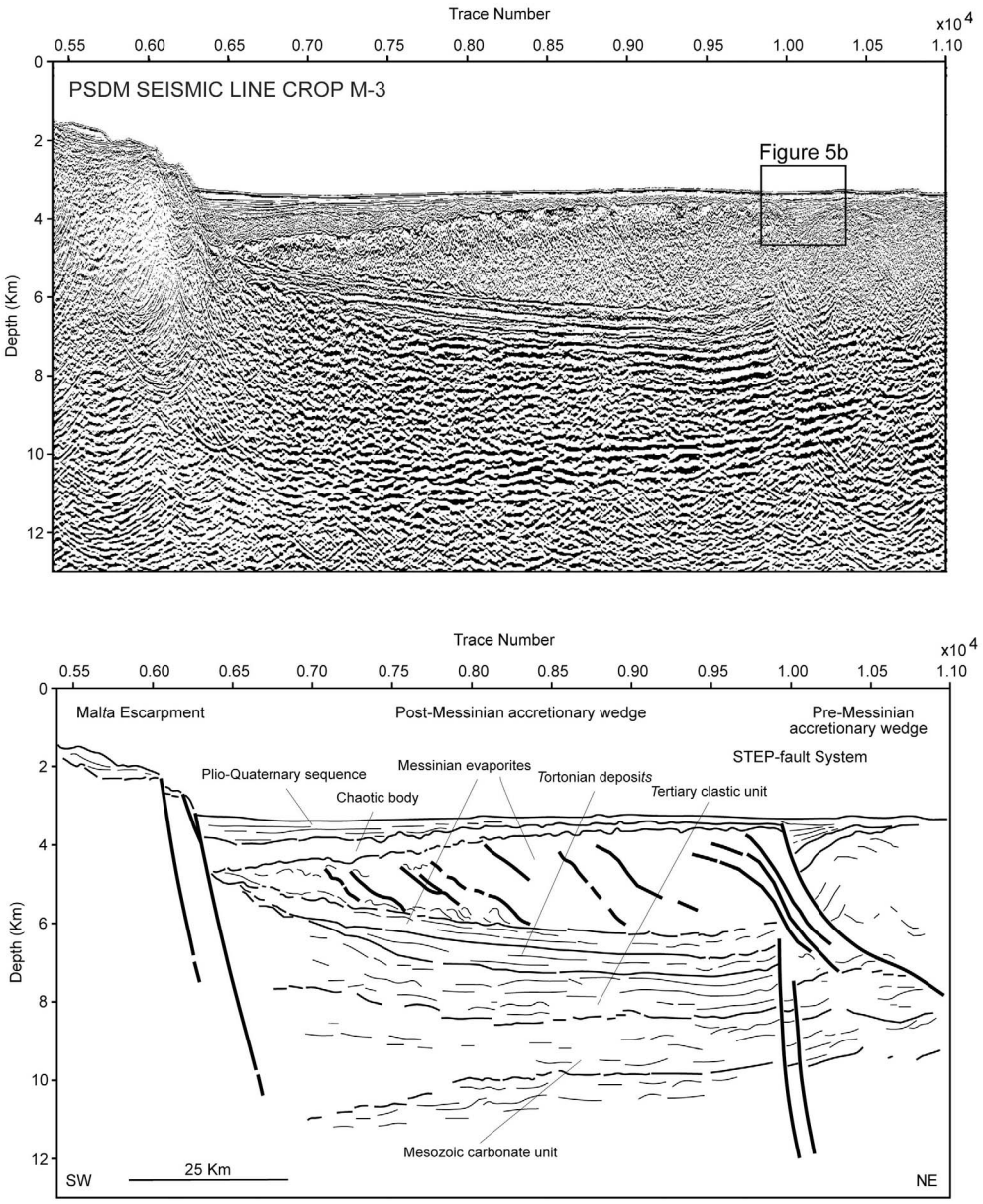

Figure 5a. Pre-stack depth migrated 36 fold MCS line CROP M-3 across the transition between the Malta escarpment and CA accretionary wedge (see Figure 2 for its location). At the toe of the Malta escarpment, the post-Messinian salt bearing complex lies on the basal detachment and is covered by a 800 m thick chaotic body representing a lower Pliocene olistostrome. At trace number 1, a lithospheric-scale fault system is imaged; this is the shallow expression of a "STEP" fault [*Govers and Wortel*, 2005]. Along this fault, large offset vertical displacement of seismic reflectors is present and a fan shaped sedimentary basin develops.

[24] We interpret this fault system as a major lithospheric structure that segments the subduction complex close to a continental corner; it may be described as the shallow expression of a "STEP" (Slab Transfer Edge Propagator) fault [*Govers and Wortel*, 2005] accommodating different rates of slab roll back and may result in substantial deformation, rotation, topography and sedimentary basins. A differential rollback between the retreating Ionian lithosphere and a "stationary" Sicilian lithosphere has also been considered by *Doglioni et al.* [2001]. The described fault represents also the boundary between the salt-bearing post-Messinian complex and the pre-Messinian clastic wedge, and is located in a region where the basal detachment cuts to deeper levels (Figure 5a). The structural features observed by *Argnani and Bonazzi* [2005] to the North support the occurrence of a lithospheric tear between the Ionian oceanic basin and the Hyblean plateau that in our opinion is represented by the lithospheric fault located at about 70 km from the Malta escarpment imaged in seismic profile M-3 (Figure 5a).

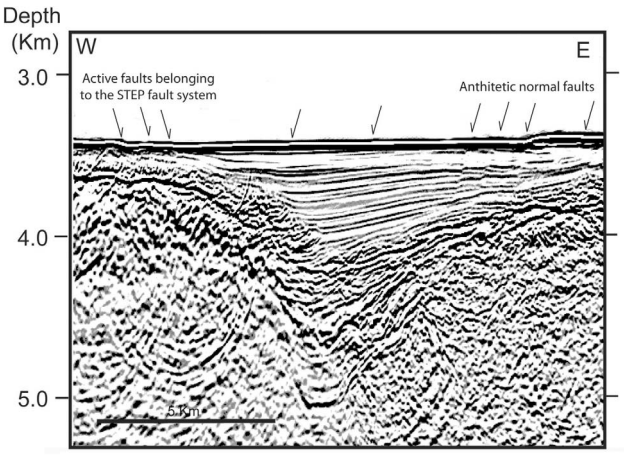

Figure 5b. Close-up view of pre-stack depth migrated 36 fold MCS line CROP M-3 seismic lien across the sedimentary basin that develops above the STEP fault. Location of seismic profile is shown in Figure 2. A series of E dipping normal faults and antithetic structures are well imaged. The seafloor appears displaced along the shallow expression of the deeply rooted lithospheric STEP fault imaged in Figure 5a.

[25] This structure plays an important role in controlling subduction processes and margin segmentation, and may represent a seismogenic feature likely to have generated major earthquakes in the past such as the 1908 Messina and 1963 Catania earthquakes. In fact, this structure is active, is large (100 km) and is deeply rooted. Moreover it bounds sectors of the margin characterized by different slip-vectors and deformation rates, and connects the plate boundary of N-Sicily to the subduction thrust of the Ionian Sea.

4. High-Resolution Seismic Reflection Data Interpretation

[26] We acquired high-resolution MCS and sub-bottom CHIRP-sonar data across the deformation front (Calamare08 survey in Figure 2); these two data sets led us to map location, geometry and nature of active structures in the outermost region of the accretionary wedge. MCS profiles were collected using an array of 2 Sodera G.I. guns as seismic source, and a 48 channels, 1200 m-long streamer as receiver. Chirp-sonar profiles were collected using a Benthos Chirp II system equipped with 15 transducers. We used these data to relate recent deformation observed at the seafloor (or in the shallow sub-surface) to deeply rooted structures, and verify whether the outer deformation front is still moving outwards as a consequence of offscraping, shortening and uplift of African plate sediments.

[27] The morpho-tectonic domains that characterize the eastern CA have also been analyzed through interpretation of a set of SPARKER seismic data (Figure 2) acquired by IGM (now ISMAR-Bo) in the Ionian Sea during the 70s [*Rossi and Sartori*, 1981]. These data, available only in hardcopies, have been digitized, processed and geo-referenced using the open-source software Seisprho [*Gasperini and Stanghellini*, 2009].

4.1. The Transition From the Ionian Abyssal Plain to the Outer Deformation Front

[28] The outermost accretionary wedge is bounded toward SE by the outer deformation front (Africa/Eurasia plate boundary in the Ionian Sea). The high resolution MCS and the CHIRP sub-bottom CALA-15 profiles (Figures 8 and 9, respectively) have been acquired close to CROP line M-2B (Figure 2), in the central part of the outermost accretionary wedge. Figures 8 and 9 show the external part of the profiles, crossing the transition between the flat Ionian Abyssal Plain domain to SE, and the outermost Calabrian wedge to NW. This is the ideal site to study active deformation driven by subduction processes. The deformation front (s.p. 1670 on the MCS profile in Figure 8 and ping 8000 on the CHIRP profile in Figure 9) marks the boundary between these two domains and is the site where the first fold affecting the seafloor is visible. A description of the observed structural domains follows.

4.1.1. The Proto-Thrust Area Under the Flat Ionian Abyssal Plain

[29] SE of the deformation front the seafloor of the Ionian abyssal plain is rather flat while P-Q and Messinian sediments are folded and deformed (Figure 8). An incipient fold is forming at about s.p. 1750, but it does not affect the seafloor, probably because the sedimentation rate is higher than uplift rate. This area belongs to the proto-thrust domain that develops at the toe of the wedge, where African plate sediments undergo the first phase of ductile deformation. Deeper reflectors show a higher degree of folding while fold amplitude progressively decreases toward SE. Folding in the proto-thrust area is related both to shortening and to halokinetic processes (i.e., salt cored folds, as fold shown at s.p. 1670 in Figure 8) driven by the differential load of the growing accretionary wedge.

[30] CHIRP sub-bottom line CALA-15 (Figure 9) collected in the abyssal plain in correspondence of the MCS profile described above, shows that incipient folds along the toe of the wedge (ping 8700 and 11300) affect the seafloor. This suggests that part of the abyssal plain deformed by incipient folding is about to be included in the accretionary wedge. We consider this region to be related to the proto-thrust domain because the seafloor appears to be only slightly undulated. Fold amplitude of deep reflectors progressively decreases from the toe of the wedge (40–50 m) to the end of the CHIRP section (10 m). Fold wavelength is rather constant, i.e., about 3 km. The relatively less deformed sediments in the proto-thrust domain are abruptly uplifted along the outer deformation front, represented by the first fold clearly disrupting the seafloor at ping 8000 (Figure 9). Deformation of the uppermost transparent layer, identified as the 3500 BP Augias Turbidite (Figure 9, ping 11000), indicates active shortening at the toe of the wedge, implying that frontal accretion is active at the wedge front.

[31] An integrated interpretation of chirp and MCS profiles shows that incipient folds in the proto-thrust domain are related to thrust faults at depth, as imaged by MCS seismic data CALA-15 at s.p. 1760 in Figure 8, where a

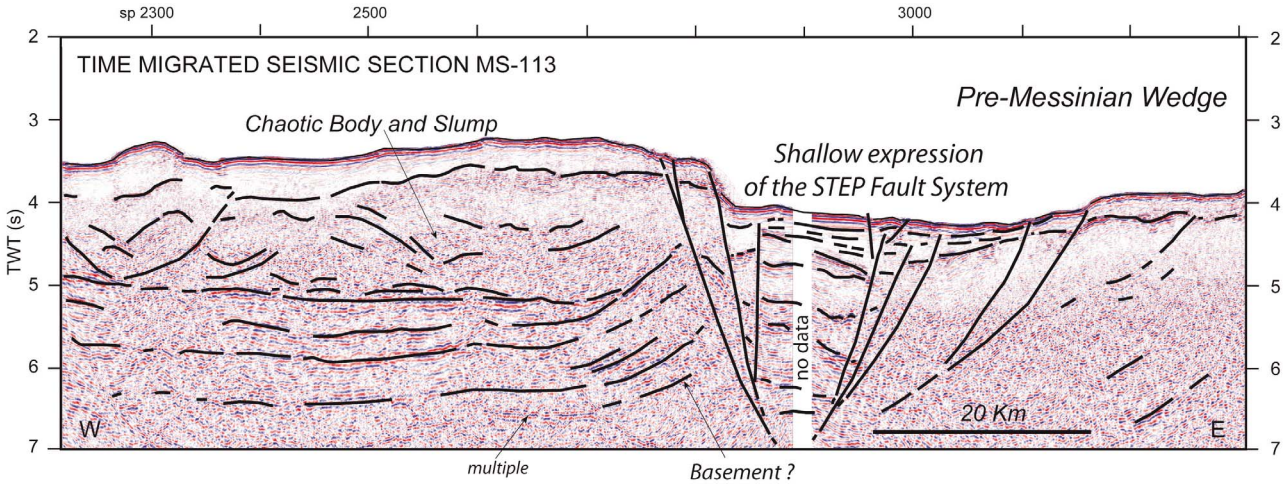

Figure 6. Post-stack time migrated MCS line MS-113 and its interpretation. This seismic profile belong to the MCS MS- data set collected by OGS (National Institute of Oceanography and Experimental Geophysics) in 1980 with a 24 traces, 2400-m-long streamer. Shot interval of 100 m provided a 12-fold coverage. Location of seismic profile is indicated in Figure 2. In this profile, the shallow expression of the "STEP" fault [*Govers and Wortel*, 2005] is particularly evident due to sedimentation rate lower than tectonic deformation rates.

landward dipping reflector soling out on the base of the Messinian evaporites appears to control the observed folding processes. Thrusting appears to be limited to the Messinian unit and to the base of the Plio-Quaternary. For this reason, we consider this part of the abyssal plain not yet fully included in the accretionary wedge. Progression of plate convergence will possibly produce a shift of the deformation front from its present position to about 4 km forward where the blind thrust fault is present (s.p. 1760 in Figure 8).

[32] Below the Messinian evaporites, a well layered sedimentary section is imaged down to 8 s TWT (Figure 8). Correlation with CROP line M-2B allow us to interpret the unconformity visible at about 7 s TWT as the base of the Tertiary section, and the prominent reflector at about 8 s TWT as the base of the Mesozoic carbonate unit.

4.1.2. The Outer Calabrian Accretionary Wedge

[33] Landward of the deformation front, the African plate sediments are deformed, uplifted and piled up to form the accretionary wedge (Figure 8), that shows the peculiar geometry (very low taper angle) of salt bearing complexes like the Mediterranean Ridge [*Chaumillon et al.*, 1996; *Chaumillon and Mascle*, 1997; *Mascle and Chaumillon*, 1998; *Reston et al.*, 2002]. The basal detachment is located at the base of the Messinian evaporites, as major thrust faults sole out on this strong amplitude reflector. This reflector appears undulated, but this is an artifact due to a seismic velocity pull-up effect. Thrust faults are mainly interpreted based on the presence of landward dipping reflectors soling out on the basal detachment, seismic reflectors offsets and small scarps at the seafloor. Thrust spacing is variable (Figure 8): it is less than 2 km landward of s.p. 1520, while seaward of this point it increases and deformation is spread over a wider area. In this weakly deformed region surface angle is about 0.5°, while the surface angle averaged from s.p. 1200 to s.p. 1680 is about 1°. Seismic resolution is poor within the accretionary wedge due to the high backscatter caused by the heavy deformation pattern.

[34] The CHIRP profile CALA-15 (Figure 9) better images the progression of folds that uplift the seafloor moving toward the inner parts of the wedge. The outermost part of the accretionary wedge (Figure 9 from ping 8000 to 14000) is characterized by a series of folds separated by perched sedimentary basins. Separation between folds and related sedimentary basin, show a characteristic 2.5 km wavelength, while the fold's amplitude, estimated considering the top

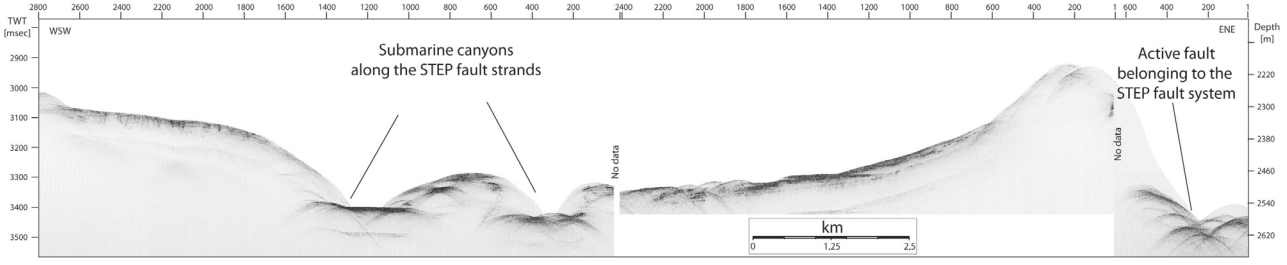

Figure 7. CHIRP sonar sub-bottom profile across the tear fault system (see Figure 2 for location). Steep topographic scarps, seafloor displacement and the presence of slumps and chaotic bodies on the flanks of the uplifted structural high to the ENE suggest that fault system is active.

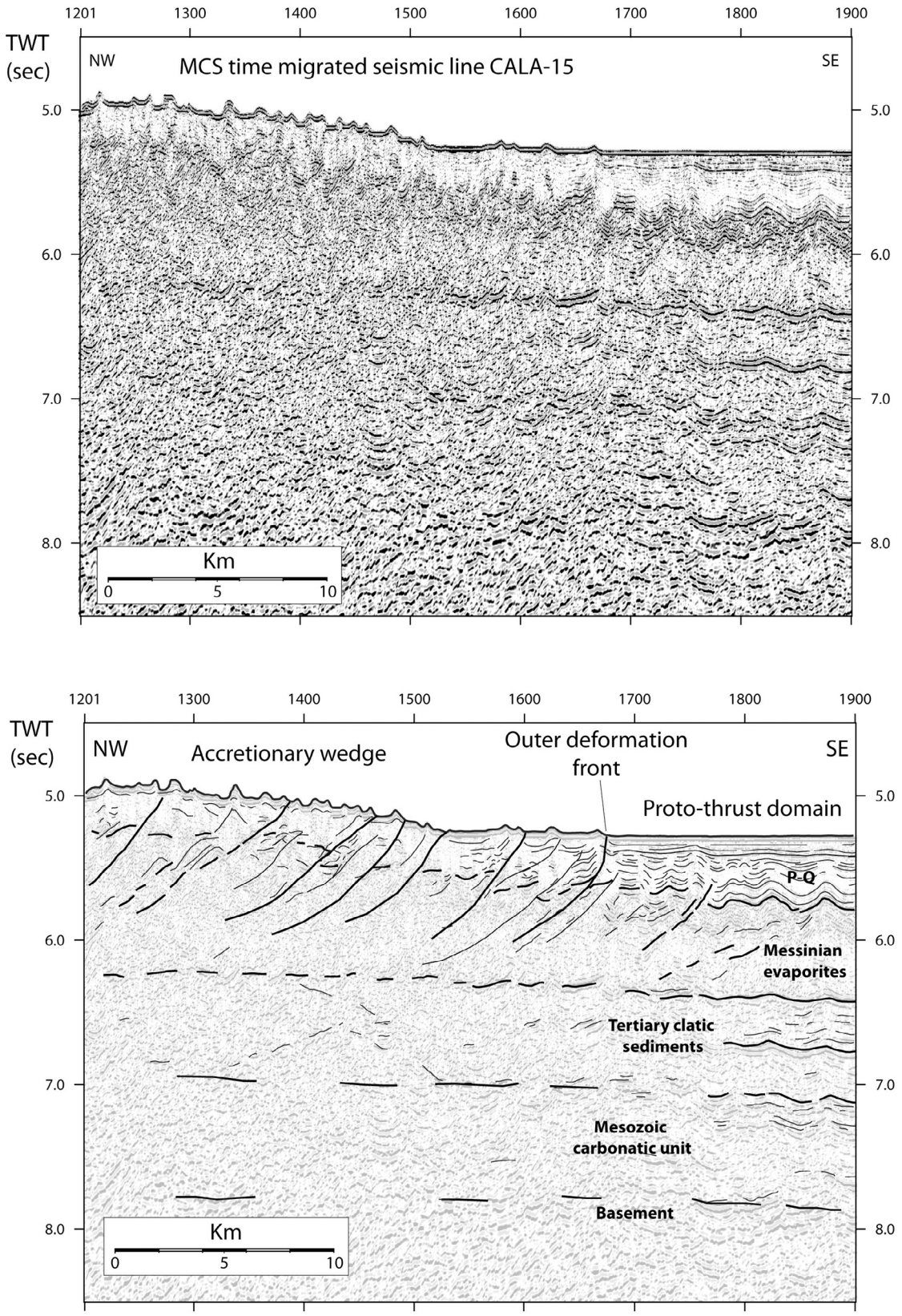

Figure 8. High resolution MCS time migrated seismic line CALA-15 across the transition between the Ionian abyssal plain and the CA accretionary wedge (see Figure 2 for location). The outer deformation front marks the boundary between the proto-thrust domain and the outer accretionary wedge. NW of the deformation front, African plate sediments are uplifted and piled up along landward dipping thrust faults soling out on the basal detachment represented by the base of the Messinian evaporites.

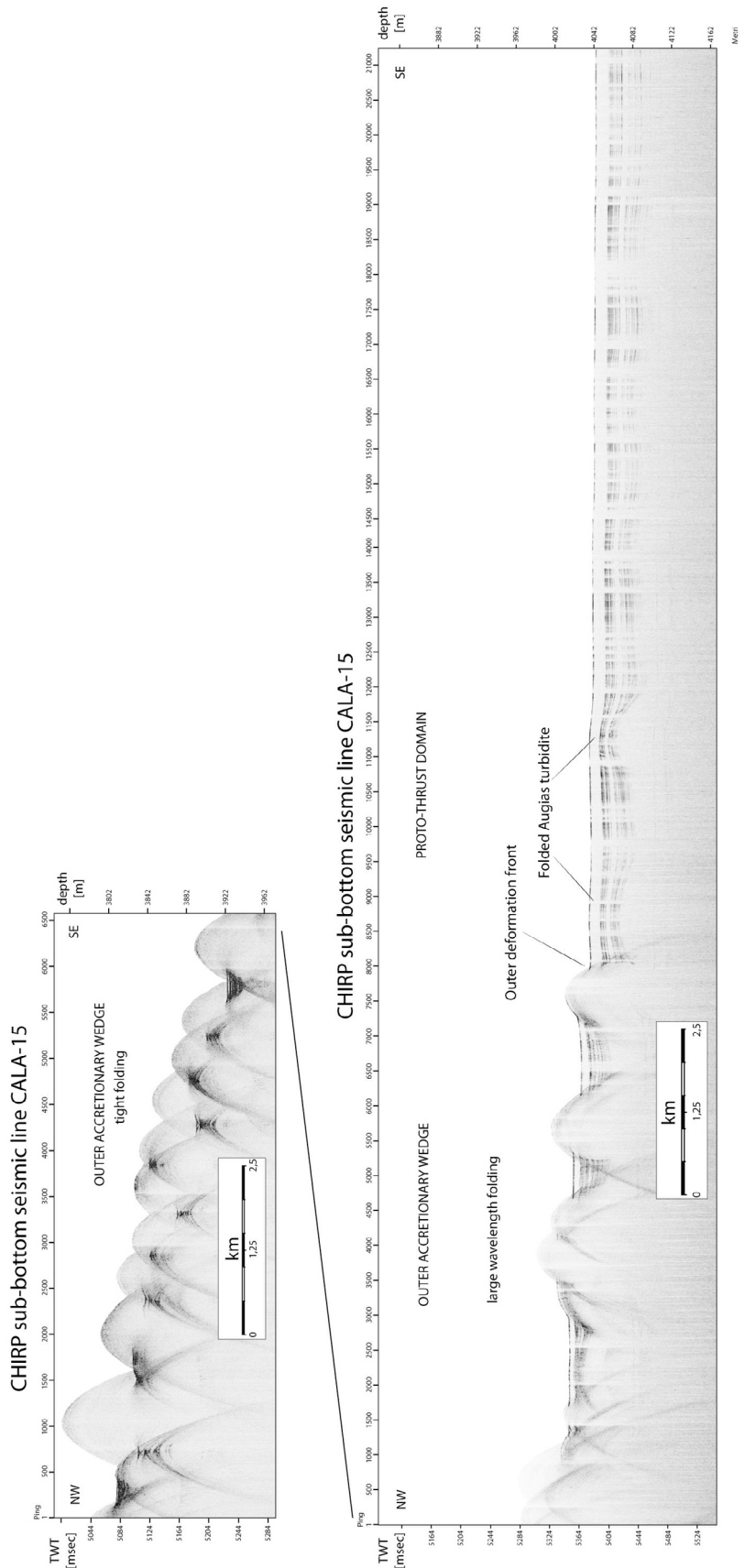

Figure 9. CHIRP sonar sub-bottom profile acquired simultaneously to the MCS profile shown in Figure 8 (see Figure 2 for location). This profile clearly shows active deformation at the seafloor related to folding and thrusting. Deformation of the uppermost transparent layer suggests that shortening is active at the toe of the wedge. Toward NW, deformation rate and fold amplitude increase, while fold wavelength progressively decreases. The rough morphology of the outer accretionary wedge is known as "cobblestone topography" and is related to tectonic processes possibly driving salt dissolution.

of the Messinian evaporites on the MCS profile (Figure 8), is about 100 m. Moving NW (Figure 9), fold spacing decreases to about 1.3–1.5 km and sedimentary basins become very narrow.

4.2. The Eastern CA and the Interference With the Mediterranean Ridge Accretionary Wedge

[35] Figure 10 shows sparker profile J-08 that crosses the continental margin from the upper slope down to about 3500 m of depth, in a region where the CA is facing directly the Mediterranean Ridge (see Figure 2 for location). It cuts orthogonally the main structures, imaging a progression of domains characterized by different seafloor morphologies and structural styles (from NW to SE, the inner plateau, the pre-Messinian wedge and the outer wedge) that have been previously described through the interpretation of CROP profile M4 (Figure 4), close to SPARKER line J-08, but not reaching the outer deformation front of the subduction system.

4.2.1. Inner Plateau: Wide Slope Terrace With a Well Developed Plio-Quaternary Sedimentary Basin

[36] It is a rather flat area dipping slightly toward SE, with large wavelength (50 km) undulations of the seafloor that develops between 1300 and 1600 m water depth. A thick section (about 1 s TWT) of Plio-Quaternary sediments is present below the terrace over Messinian deposits whose top is located at about 2.3 s TWT at fix 85 (Figure 10), as confirmed by well-log data (Floriana borehole). Sediments appear folded and locally disrupted along sub-vertical deformation zones that bound sedimentary units characterized by transparent seismic facies (fix 83 and 84) corresponding on the seafloor to small (about 1 km wide) sub-circular swells, probably of diapiric origin. The nature and composition of the diapiric material (mud or evaporites) is not determined through seismic data, but correlation with an exploration borehole well log (Floriana, Figure 2 for location) suggests they might be evaporite-cored diapirs as the well log has sampled the Gessoso Solfifera Formation (crystalline white gypsum, anhydrite, clay layers with salt). The source region of these diapirs is in fact located at about 2.2–2.3 s TWT, where the Messinian unit is visible (Figure 10). Interestingly, the Messinian unit appears to thin toward the diapiric structure, possibly as a result of lateral flows. Immediately SE of fix 70 and close to the sub-vertical fault described at fix 71, another mound is present. Its geometry and location suggests it might be an argilo-kinetic structure, since it develops in a region where the Messinian salt or gypsum are absent. Diapiric processes observed in this region might be related to the presence of transtensive faults segmenting the continental margin [*Del Ben et al.*, 2008], similar to those controlling development of the Squillace Basin. Sparker section J-03 crossing this basin images a NE dipping master fault outcropping at the seafloor at fix 21, which appears to drive diapiric processes (Figure 11). The external part of the inner plateau is site of a 300 m deep sedimentary basin (Figure 10, fix 61–63) that shows a flat bottom and a sub-horizontal Plio-Quaternary infill.

4.2.2. Inner Wedge

[37] This is a region characterized by a progression of long wavelength (about 10 km) and high amplitude (about 250–300 m) undulations of the seafloor. In sparker line J-08, between fix 53 and fix 39 (Figure 10) a depressed area below the regional topographic profile is present, with two deep sedimentary basins separated by structural highs. The depressed area is bounded to the NW by a seaward dipping topographic scarp (Calabrian Escarpment), along which the seafloor deepens of about 1 s TWT (750 m). In the bathymetric map (Figure 1) this scarp corresponds to a NNE-SSW trending sub-rectilinear feature that separates longitudinally the pre-Messinian wedge from the rather flat inner plateau to the NW. The pre-Messinian wedge is bounded to SE by the inner deformation front (Figure 10) separating the pre- and post-Messinian accretionary wedges. This part of the subduction complex has been described by *Rossi and Sartori* [1981] as the "external CA." In our reconstruction, the so-called "external CA" represents the inner accretionary wedge emplaced during pre-Messinian times.

4.2.3. Outer Wedge and Transition to the Mediterranean Ridge

[38] The outer wedge is characterized by a very poor seismic penetration on the sparker data (Figure 10). A rough seafloor morphology is related to the presence of close-spaced folds superimposed over large wavelength undulations that produce several kilometers wide alternating depressions and highs. This seafloor texture appears different from the post-Messinian wedge morphology typical of the western CA, where fold spacing is very narrow and no large basins are present. The integrated interpretation of SPARKER line J-08 (Figure 10) and MCS line CROP M-4 (Figure 4) suggests that the depressions imaged in SPARKER profile J-08 are the morphological expression of the duplex structures that involve the whole sedimentary section in this portion of the subduction complex (Figure 4). Sparker profile J-08 (Figure 10) images the area where the CA connects to the Mediterranean Ridge accretionary complex. This transition is located at about 3000 m water depth: no undeformed abyssal plain is present, and the two accretionary wedges connect, suggesting that incipient collision is occurring between the two subduction complexes. The SPARKER profile has no penetration; thus, this seismic line does not unravel interference patterns of the two colliding subduction complexes.

5. Discussion

5.1. Across Strike Regional Architecture and Active Faults

[39] The frontal region of the CA complex is formed by a post-Messinian accretionary wedge made of Messinian evaporites overlain by Plio-Quaternary, extensively folded, hemipelagites and turbidites. The basal detachment of the wedge occurs at the base of the Messinian evaporites: above the basal detachment sediments have been offscraped and piled up in the accretionary wedge through frontal accretion while the pre-Messinian sediments are attached to the underlying African plate. The salt-bearing accretionary wedge in the western CA is bounded toward the NW by a slope terrace located at about 3000 m water depth. This flat area has been interpreted by many authors as the seaward boundary of the CA subduction complex and the outer deformation front has been often reported along the landward edge of this terrace [*Rossi and Sartori*, 1981; *Frepoli et al.*, 1996; *Catalano et al.*, 2001; *Faccenna et al.*, 2001; *Bigi et al.*, 2003; *Goes et al.*, 2004; *Chiarabba et al.*, 2005; *Govers and Wortel*, 2005; *Lucente et al.*, 2006; *Minelli and*

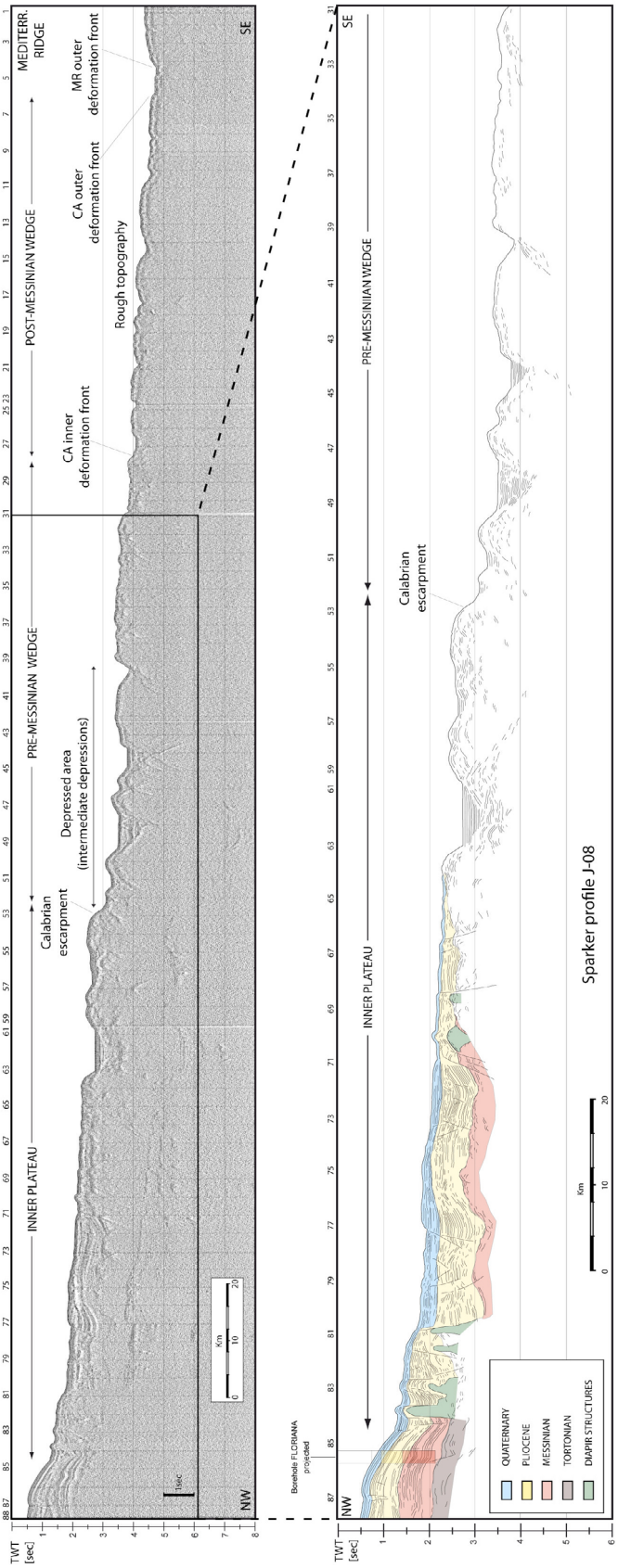

Figure 10. Sparker seismic profile J-08 across the continental margin south of Calabria (see Figure 2 for its location). This profile highlights the different seafloor morphology related to the progression of structural domains that characterize the CA subduction complex in this region. The rather flat inner plateau is bounded toward S by the rough morphology of the inner accretionary wedge, and by a gently folded outer accretionary wedge facing directly the Mediterranean Ridge accretionary complex. Correlation between seismic and borehole data allow to identify and date main seismostratigraphic units.

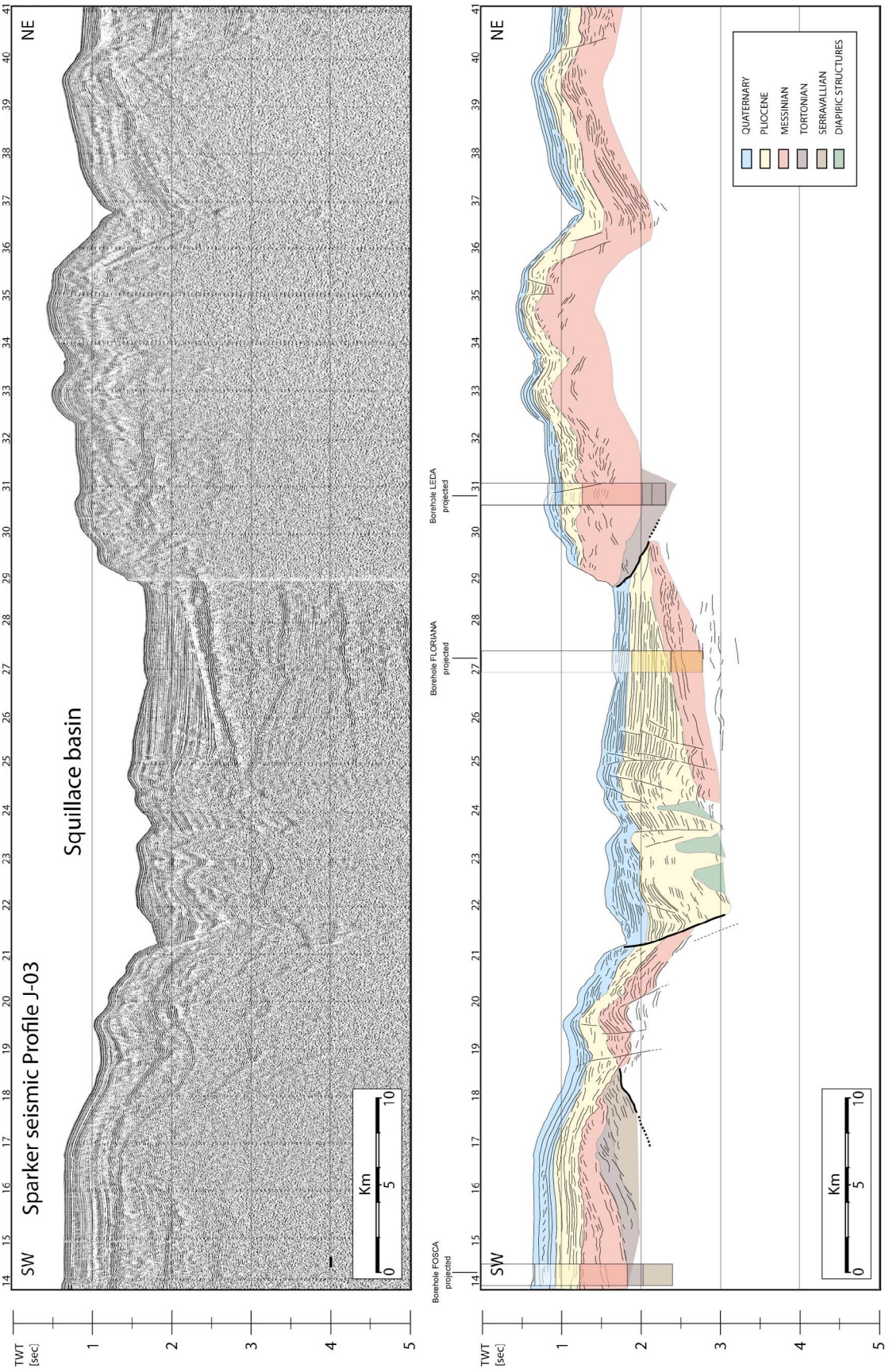

Figure 11. Sparker seismic profile J-03 parallel to the Calabrian continental margin (see Figure 2 for location). The profile clearly shows a sub-vertical normal master fault controlling the development of the Squillace basin to the SW, and the reverse fault bounding the sedimentary basin to the NE. Diapiric structures are present within the hanging wall of the normal fault.

Faccenna, 2010] or even within the post-Messinian wedge [*Guillaume et al.*, 2010].

[40] The integrated interpretation of our multiscale data set has clearly shown that the frontal thrust is located indeed at the transition with the abyssal plain. Moreover, the very low tapered salt-bearing wedge landward of the deformation front is still growing thanks to frontal tectonic accretion occurring at the base of the lower Messinian evaporites (Figures 3a, 8, and 9). The flat area at the rear of the salt-bearing complex in the western region (Figures 3a and 3b) corresponds to a thrust top Messinian basin developing at the transition between the salt bearing complex and pre-Messinian wedge. Below the sedimentary basin, the basal detachment cuts to deeper levels. This may lead to the development of duplex structures, subcretion and underplating of pre-Messinian sediments, similarly to what has been described for the Mediterranean Ridge to the East [*Reston et al.*, 2002]. Moving from SE to NE in this region, the subduction thrust changes its dip from a rather flat geometry to about 4° of slope, and CROP seismic lines image out-of sequence thrusts, that propagate down to the top of the subducting plate (Figures 3a and 3b). In the Eastern region (Figure 4) detachment level variations occur in a front-most area, within the salt bearing accretionary wedge, and also in this region where the detachment gets deeper a number of out of sequence thrust faults (splay) develop to accommodate depth variations.

[41] These faults reflect, on one hand the structural contrast between a shallow décollement (base of the Messinian evaporites) in the frontal wedge and a deep décollement within the innermost accreted sediment; on the other hand, they may be expression of underplating occurring at depth, where the thick Tertiary and Mesozoic sediments are incorporated at the base of the accretionary wedge. An accurate knowledge of geometry and degree of activity of these faults is important to estimate more accurately seismic and tsunami hazard. In fact, splay faults have been proposed as pathways for co-seismic slip, which can potentially increase the amplitude of an associated tsunami [*Cummins and Kaneda*, 2000; *Park et al.*, 2002; *Satake et al.*, 2003; *Sibuet et al.*, 2007]. IODP drilling results along the Nankai margin, for example, highlight that, despite the western portion of the splay fault has been inactivated since 1.24 Ma by the collision with a seamount [*Kimura et al.*, 2011], the eastern portion of the splay fault has remained active since the inception of faulting (shortening rate 1 m/kyr) and the authors conclude that branches of the megasplay fault may slip and deform coseismically [*Kimura et al.*, 2011] and orientation and geometry of the fault are keys to evaluate the activity.

[42] The pre-collisional tectonic setting of the Ionian Sea is characterized by a strong geological complexity mainly related to the irregular plate boundary, different rates of deformation and variations in the structure and nature of the incoming African lithosphere. In this pre-collisional setting the described splay faults may represent active fault absorbing plate motion even though deep-towed geophysical data, well targeted sediment samples, ROV observations and drilling are crucial to evaluate splay fault activity. If subduction in the CA is still active they may represent subduction megathrusts and may slip and deform coseismically, especially those branches in the eastern area offshore Calabria (Figure 4) where the subducting lithosphere remains undetached as deduced by local earthquake tomography [*Neri et al.*, 2009]. If subduction is already ceased and the prism is not deforming by underthrusting of an oceanic plate but, rather, by a more distributed deformation, the proposed splay faults may represent reactivated thrust faults absorbing ongoing plate convergence in an overall plate re-organization tectonic phase. As in the case of other active margins, forearc basins and slope terraces like the one present in the CA above the splay faults, are often linked to changes in the dip of the subduction thrust and related syn-tectonic sedimentation; as observed in several regions including Nankai, Aleutians and Cascadia, gravity lows and deep sea basins may represent regions more prone to seismic risk [*Wells et al.*, 2003; *Fuller et al.*, 2006].

[43] The boundary between the pre-Messinian wedge and the inner plateau in the eastern region occurs along the Calabrian Escarpment present at about s.p. 2500 in Figure 4 that corresponds to splay-3 described on the high penetration MCS data. This feature shows all the characters of a transpressive fault accommodating strain partitioning at the contact between the wedge and the inner plateau. A similar setting is observed in the Mediterranean Ridge accretionary complex, where the accretionary wedge/backstop contact is represented by major strike slip faults [*Chaumillon and Mascle*, 1997; *Mascle and Chaumillon*, 1998; *Chamot-Rooke et al.*, 2005b]. These structures are often associated with fluid venting because they represent conduits along which material coming from the wedge interior can be extruded to the seafloor forming argilo-kinetic structures. The lack of the evaporitic impermeable cap, active faulting along the inner deformation front and transverse structures segmenting the subduction complex, are all elements that favor rising of fluids from the wedge interior and formation of diapiric features [*Chamot-Rooke et al.*, 2005a]. The recently discovered Pythagoras mud diapir [*Praeg et al.*, 2009] is located along the wedge/inner plateau tectonic contact, confirming that this boundary represents a favorable pathway for rising fluids.

5.2. Seafloor Morphology of the CA as Deduced From Multibeam Data

[44] If on one hand, the CA has always been described as a single arc developed between the Malta escarpment and Apulia foredeep, MCS data analysis has shown that the geometry of the subduction complex (width, thickness, elevation, depth of the basal detachment) and its structural style strongly vary along strike. Analysis of the morphobathymetric data collected during different cruises carried out in the Ionian Sea and provided by the CIESM/Ifremer Medimap group [*Loubrieu et al.*, 2008] confirms that major morphotectonic style variations occur between the western and the eastern sectors of the CA (Figure 12), suggesting segmentation of the subduction complex into two separate domains, we call Eastern Lobe (EL) and Western Lobe (WL).

[45] The EL has a very arcuate shape that progressively narrows to the SE where it impinges against the Mediterranean Ridge and no abyssal plain is present (Figure 12, profile a). A very complex seafloor morphology develops at the contact between the CA and MR subduction complexes (between 4000 and 3750 m water depth) where short

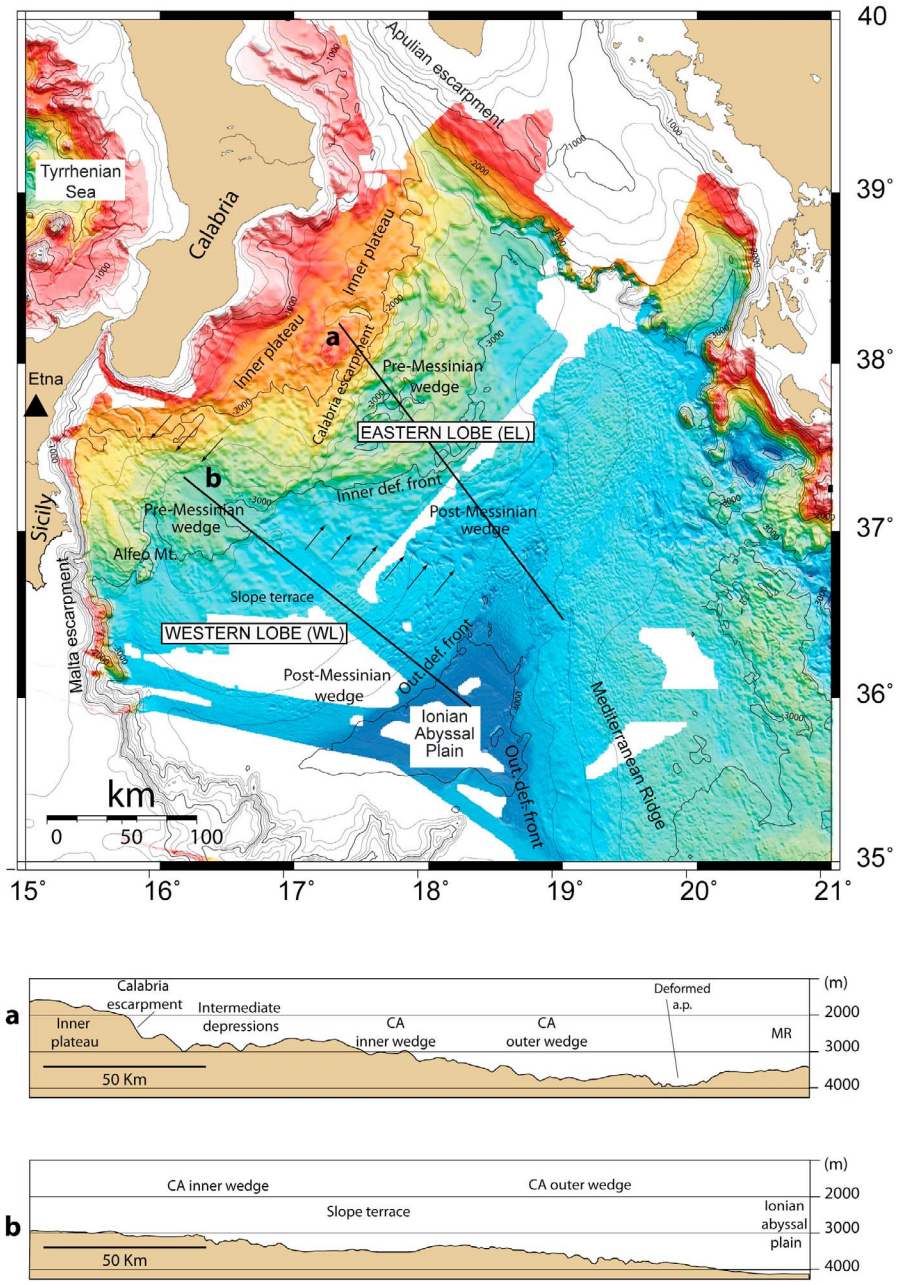

Figure 12. Shaded relief morphobathymetric map compiled using data collected during different cruises by the CIESM/Ifremer Medimap group [*Loubrieu et al.*, 2008]. Major morphotectonic domains are indicated. The margin is segmented into two lobes (WL and EL). The boundary between the two lobes (black arrows) is marked by a diffuse area of deformation related to scarps, ridges and troughs. Two bathymetric profiles (a and b) across the two lobes highlight morphological differences.

(≈1 km) wavelength depressions and swells develop, possibly related to small-scale, tectonically triggered halokinetic processes. The outermost accretionary wedge in this region shows a rough morphology with ridges and troughs with few km wavelength (Figure 12, profile a). To the rear of the 3000 m isobath topographic slopes get steeper, up to the upper part of the wedge (outer high) while backward a depressed area is present (intermediate depressions of *Rossi and Sartori* [1981]). These depressions belong to the inner wedge that corresponds to the pre-Messinian clastic accretionary wedge as deduced from the interpretation of seismic line CROP M4 (Figure 4).

[46] The intermediate depressions are bounded to the NW by the Calabria Escarpment, a prominent feature segmenting longitudinally the subduction complex, previously described on the basis of MCS data. The geometry of the Calabrian Escarpment, as deduced from the multibeam data (i.e., a series of short and overlapping left stepping scarps) suggests it represent a transpressive feature bounding the accretionary

wedge to the NW. Inward of the Calabria Escarpment, a rather flat area is imaged (i.e., the inner plateau).

[47] The WL is a very wide fan-shaped lobe, which reaches its maximum width and curvature at the contact with the abyssal plain at about 4000 m water depth; it narrows toward land, and loose its curvature north of the Alfeo seamount. Profile b in Figure 12, shows that the outer accretionary wedge is characterized by very gentle slopes and a rough topography, due to the presence of depressions and swells whose wavelength increases toward NW. The outer accretionary wedge is wider than in the EL and bounded landwards by a 40 km wide slope terrace, that corresponds to the region where the out of sequence thrust faults are imaged on the CROP line M-2B (Figure 3a). The Pre-Messianian wedge developing NW of the slope terrace is a complex region that shows deeply incisions related to multiple systems of submarine canyons, wide depressions and transverse topographic highs. The outer high in the WL is located within the outer ridge while in the EL is located landwards at the contact between the inner wedge and the intermediate depressions. The comparison between the profiles across the two distinct lobes (Figure 12, profiles a and b) clearly shows that the eastern lobe is steeper, more elevated and with swells and depressions characterized by larger amplitudes and wavelengths.

[48] The integrated interpretation of MCS data and multibeam images suggests that differences in seafloor morphology are related to deep tectonic processes and possibly to different coupling rates on the plate boundary and recent plate re-organization as described in the following section.

5.3. Along-Strike Segmentation of the Subduction Complex

[49] We carried out an integrated interpretation of multiscale seismic reflection profiles combined with available morphobathymetric data (Figure 12) in order to describe structural style variations along the accretionary wedge, and associate these variations to tectonic processes. The results are summarized in the structural map of the region (Figure 13) which includes major structural boundaries, active faults and the extent of the different structural domains (i.e., pre and post-Messinian wedges and inner plateau).

[50] The Western Lobe (WL) develops at the toe of the Malta escarpment and extends southwards down to the −4000 m isobath. Here, the subduction complex shows its maximum extension and is fronted by a wide abyssal plain domain. The WL architecture is imaged in seismic line CROP M-2B (Figure 3a) and is characterized by a typical low tapered accretionary wedge detaching on the base of the Messinian evaporites.

[51] The accretionary wedge is still growing through frontal accretion and the upper part of the incoming African plate sedimentary section is scraped off and piled up along seaward dipping thrust faults, soling out to the base of the Messinian evaporites. The lithospheric structure we recognized through the analysis of CROP line M-3 (Figure 5a), 70 km East of the Malta escarpment (STEP fault in Figure 13), has been previously described by *Chamot-Rooke et al.* [2005b] as a Mesozoic crustal-scale structure marking the continent-ocean boundary of the Ionian oceanic basin and presently still active with a near-vertical step-like motion. Although these authors suggested it may represent the western boundary of the Calabrian wedge, our data (Figure 5a) show that the post-Messinian salt bearing accretionary wedge is present also west of this structure. This implies that this fault does not represent the western boundary of the accreted sediments, but rather it displaces vertically the top of the accretionary wedge and deeper reflectors. It was probably active throughout the Plio-Quaternary, as testified by the syn-tectonic sedimentation within the sedimentary basin that develops above it (Figures 5b and 6). This fault may represent a transtensive re-activation of the Messinian subduction thrust fault between the pre and post-Messinian wedge presently acting as a STEP fault between regions with varying slab dynamics.

[52] The Eastern Lobe (EL) develops offshore Calabria in front of the western verging Mediterranean Ridge and is represented by seismic line CROP M-4 (Figure 4). In this region no undeformed abyssal plain is imaged as the two opposite verging accretionary wedges are facing each other producing complex interference deformation patterns. No slope terrace develops between the pre and post-Messinian accretionary complexes. The accretionary wedge is narrower and it shows a very lobate shape, well represented by outer and inner deformation fronts (Figures 4, 10, and 13). Seismic images reveal a deeper décollement in this region, while wedge geometry and structural style (width, surface slope, fold wavelength and amplitude) suggest higher shortening and uplift rates, possibly related to varying rates of plate coupling on the basal detachment. In this region, in fact, the presence of basement involved deformation and duplex structures suggest the occurrence of underplating processes also in the frontal part of the wedge.

[53] We interpret these two lobes as related to two distinct stages of the subduction processes, different rates of slab roll back or slab dynamics and plate fragmentation in the Ionian Sea. The Ionian Sea region represents the final stage of the closure of an oceanic basin characterized by very irregular continental margins and the presence of continental promontories. We have described and mapped active tectonic structures in different regions of the subduction complex (i.e., wedge front, splay faults below the slope terrace, inner deformation front and Calabria Escarpment). Recent deformation may be either interpreted as related to the last stage of Calabria subduction and/or to the ongoing Africa/Eurasia plate convergence that may occur without a slab penetrating into the mantle.

[54] A combined analysis of deep seismic profiles, gravity and earthquake tomography data, as well as numerical and analog modeling derived from these geological constraints, will help understanding how the shallow structure of the subduction complex is related to deeply rooted tectonic processes and if a new plate re-organization is going on in this area.

[55] The major tectonic boundary delimiting the two proposed lobes of the accretionary wedge (Figures 13) has been studied through the analysis PSDM MCS line M-3 represented in Figure 14 that shows a wide area of deformation between the two proposed lobes producing displacements, and tectonic thickening of the deep units (i.e., Mesozoic carbonates and basement) as well as deformation of the upper units with the formation of a series of ridges

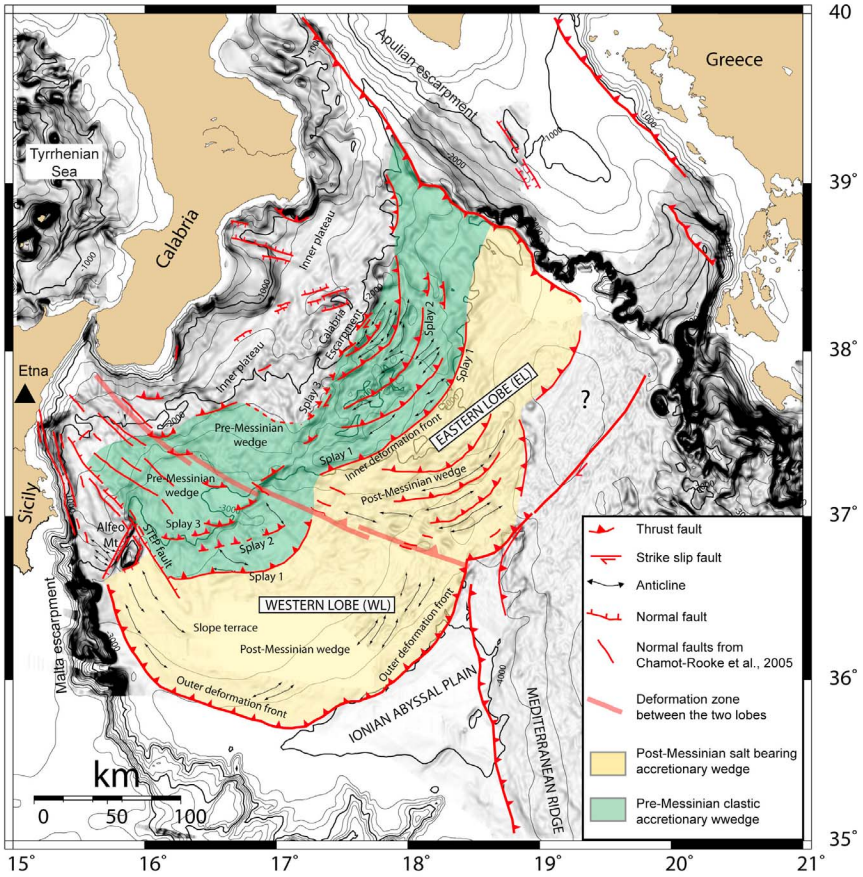

Figure 13. Structural map of the CA region derived from integrated interpretation of available seismic data and multibeam bathymetry provided by the CIESM/Ifremer Medimap group [*Loubrieu et al.*, 2008] superposed over a gray levels bathymetric slope map. Major structural boundaries, active faults and the extent of the structural domains (i.e., pre and post-Messinian wedges and inner plateau) are indicated. The continental margin is segmented both across and along strike. The STEP fault located at about 70 km east of the Malta Escarpment and the splay faults (splay 1, 2 and 3) are considered active features likely to have generated major earthquakes in the past. The diffuse structural boundary between EL and WL accommodates different rates of shortening, slab rollback and subduction dynamics in the different segments of the CA subduction zone.

and troughs at the seafloor well visible on the multibeam map of the study area (Figure 12). The diffuse area of deformation is related to low angle, eastward dipping faults along which the eastern lobe is overriding the western domain. To the North, close to the Messina strait this structural boundary is more likely represented by the set of transtensive faults well described at the toe of the Malta escarpment by *Chamot-Rooke et al.* [2005b]. This transtensive fault system, displaces longitudinally the subduction complex and create a depressed area East of Sicily, also visible in the satellite-derived free-air gravity map of the region (Figure 15) that shows two different patterns in the EL and the WL, separated by a linear gravity minimum corresponding to the deformed region between the two lobes imaged in Figures 13 and 14.

[56] Along this structural system relevant changes in direction of GPS velocities are imaged between sites in Sicily with respect to those in Calabria [*Devoti et al.*, 2008; *D'Agostino et al.*, 2008]. This suggests that the boundary we propose between the WL and EL represents the expression of a differential advance between the "true Calabrian" and Peloritan portions of the CA, explaining both the NW-SE extension in the straits of Messina [*D'Agostino and Selvaggi*, 2004] as well as why Calabria is a bit offset (it appears to have advanced further SE) from NE Sicily. This differential offset would require a lithospheric scale fault between Calabria and NE Sicily while its primary expression within the wedge would be a sort of transfer fault.

[57] Major structural heterogeneities described in seismic profiles, and the overall segmentation of the subduction complex in two lobes, may represent the shallow signature of deeply rooted process and plate fragmentation in an incipient collisional setting at the end of the subduction phase. In fact, the distributed deformation described in the region between the two lobes corresponds to the transition between segments of the plate boundary where the slab is already detached (northeastern Sicily) and the 100-km-long segment of southern Calabria where the subducting lithosphere remains undetached as deduced by local earthquake tomography [*Neri et al.*, 2009].

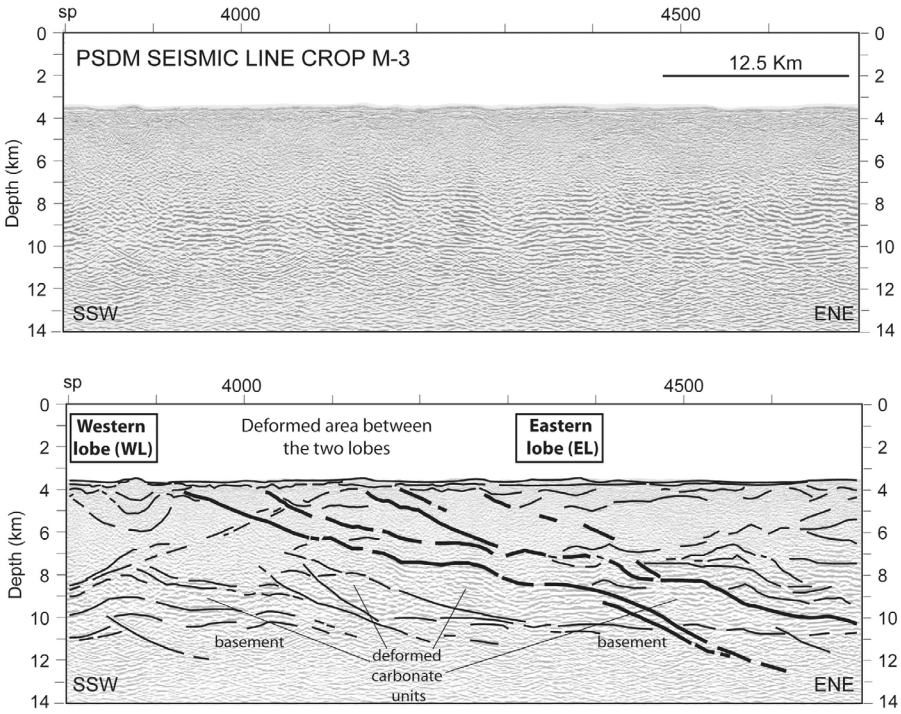

Figure 14. Pre-stack depth migrated MCS line CROP M-3 crossing the boundary between the two proposed lobes of the subduction complex. A wide and diffuse area of deformation is observed between the Western and Eastern lobes where displacement of the deep units (i.e., Mesozoic carbonates and basement) is accompanied by the formation of a series of ridges and troughs at the seafloor.

5.4. Post-Messinian Kinematics and Comparison With the Mediterranean Ridge

[58] The overall geometry of the subduction complex (depth of the basal detachment, thickness and extension of the accretionary wedge), as revealed by CROP M-2B profile (Figure 3a), has been used to reconstruct rates of sediment accretion and long-term plate convergence. The geometry of the CA accretionary wedge (alpha and beta angles) in seismic line CROP M-2B implies that this wedge is in the typical accretionary stability field, similarly to the Nankai, Barbados and Mediterranean Ridge accretionary complexes. These wedges' very low topographic slopes and beta angles fall in the unstable compressional field of the stability diagram of critical wedges [*Lallemand et al.*, 1994]. Simple area balancing estimates made on this seismic section allowed for reconstructing the volume per unit section of sediments emplaced in the wedge. If, according to stratigraphic and geophysical constraints, the salt-bearing accretionary wedge has been emplaced during and after the Messinian salinity crisis (5 Ma), and we assume that the outer deformation front was located during Messinian time at the contact between the pre- and post-Messinian wedges (about 100 km landwards of its present location), the rate of outward movement of the deformation front should be in the order of 2 cm/yr. This value is comparable to that proposed for the Mediterranean Ridge by *Kastens* [1991] through analysis of sediment facies within the wedge. The rapid rate of outward growth is reflected in the very low taper angle (1–1.5°) that might be explained by the mechanical strength of the evaporites over a very weak basal detachment that favors outward growth rather than vertical stacking of accreted units. In any case, the rate of outward growth derived from seismic section is more rapid than the current African/Eurasian plate convergence. The same discrepancy has been reconstructed in other subduction complexes such as the Barbados wedge where *Le Pichon et al.* [1990] estimated that outward wedge velocity changed rapidly through time, and that the accretionary complex progressed much faster than the subduction rates in the first few millions of years of subduction history [see *Le Pichon et al.*, 1990, Figure 7a].

[59] The Messinian salinity crisis may be seen as a dramatic event that has caused the beginning of a new subduction cycle in the whole Mediterranean Sea. The Messinian abrupt sea level variations and the rapid syntectonic deposition of very thick evaporites in the Mediterranean Sea may have produced an abrupt change in the geometry of the evolving submarine subduction complex, leading to changing stability conditions of the wedge itself. This sharp transition should have changed the stability conditions of the CA wedge that may have moved from a critical state to an unstable compressional regime. Moreover, flexural rebound following the Messinian sea level drop caused an uplift of the toe of the wedge and the relative decrease of the surface slope caused the wedge to become subcritically tapered and deformation shifted to the internal part of the wedge to restore taper to critical value [*DeCelles and Cavazza*, 1995]. Latest Miocene-Pliocene marine inundation reloaded the basin and we can argue that a very fast outward growth of the prism resumed to restore the wedge to the new critical state facilitated by the presence of

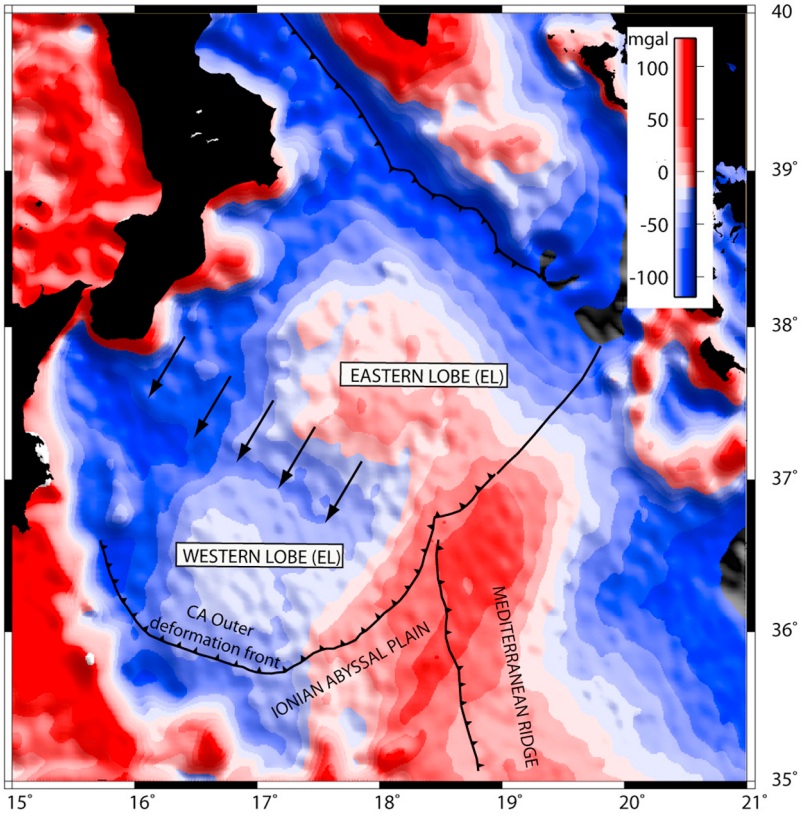

Figure 15. Free-air satellite-derived gravity map of the working area. Eastern and Western lobes (EL and WL) are characterized by the presence of two bulges separated by a NW-SE trending gravity minimum (black arrows) corresponding to the wide deformed area between the two lobes imaged in seismic reflection (Figure 14) and morphobathymetric data (Figures 12 and 13). Average difference in the gravity field between the two lobes exceeds 100 mgal.

the very weak basal detachment on the Messinian evaporites. If this reconstruction is correct, a very intense phase of accretion resumed during Messinian times aiming at reaching again the stability curve. In this reconstruction wedge building is not a linear process and a large part of the CA post-Messinian accretionary wedge may have been emplaced during or immediately after Messinian times.

[60] To better analyze relationships between frontal accretion and convergence rate we carried out a cross-sectional area balancing on the depth-converted seismic section CROP M-2B (Figure 16a). The long-term accretionary history can be estimated comparing the volume per unit section of the post-Messinian wedge (its area on the seismic profiles) and the sediment input in the trench during the last 5 Ma (i.e., the product of the integrated amount of orthogonal convergence during the post-Messinian wedge building and the thickness of sediment entering the subduction zone). Sediment input S is

$$S = CV * T * TH \quad (1)$$

where CV = convergence velocity, T = time = 5 Ma and TH = thickness of the sedimentary section above the basal detachment. Substituting real values in (1) gives 32 km^2 of sediments available for accretion during the last 5 Ma within those stratigraphic and kinematic constraints.

[61] The area (A) of the post-Messinian wedge on seismic line CROP M-2B, is given by

$$A = {}^1\!/_2(H + h) * L$$

where L is the width of the salt bearing wedge (about 100 km), and h and H its thickness in the abyssal plain (about 1.5 km) and in its landward boundary (about 3.5 km). This gives a volume per unit section (area) of about 250 km^2 (Figure 16a).

[62] As a consequence, the estimated volume per unit section of the salt bearing accretionary complex in our seismic line is about 7 times larger than the volume of sediments entering the trench at the given convergence rate (0.5 cm/yr). This simple estimate assumes a constant thickness of Messinian evaporites in the abyssal plain, no variation in basal detachment depth and no volume loss during accretion. On the other hand, the volume per unit section of the CA post-Messinian wedge is comparable to that of the Mediterranean Ridge where convergence rate is on the order of 3–4 cm/yr [*Chaumillon et al.*, 1996; *Mascle and Chaumillon*, 1998; *Reston et al.*, 2002].

[63] This discrepancy may be explained by different causes that are not mutually exclusive.

[64] 1. Convergence rate slowed down in the CA only in the past one or two million years. This explanation is in

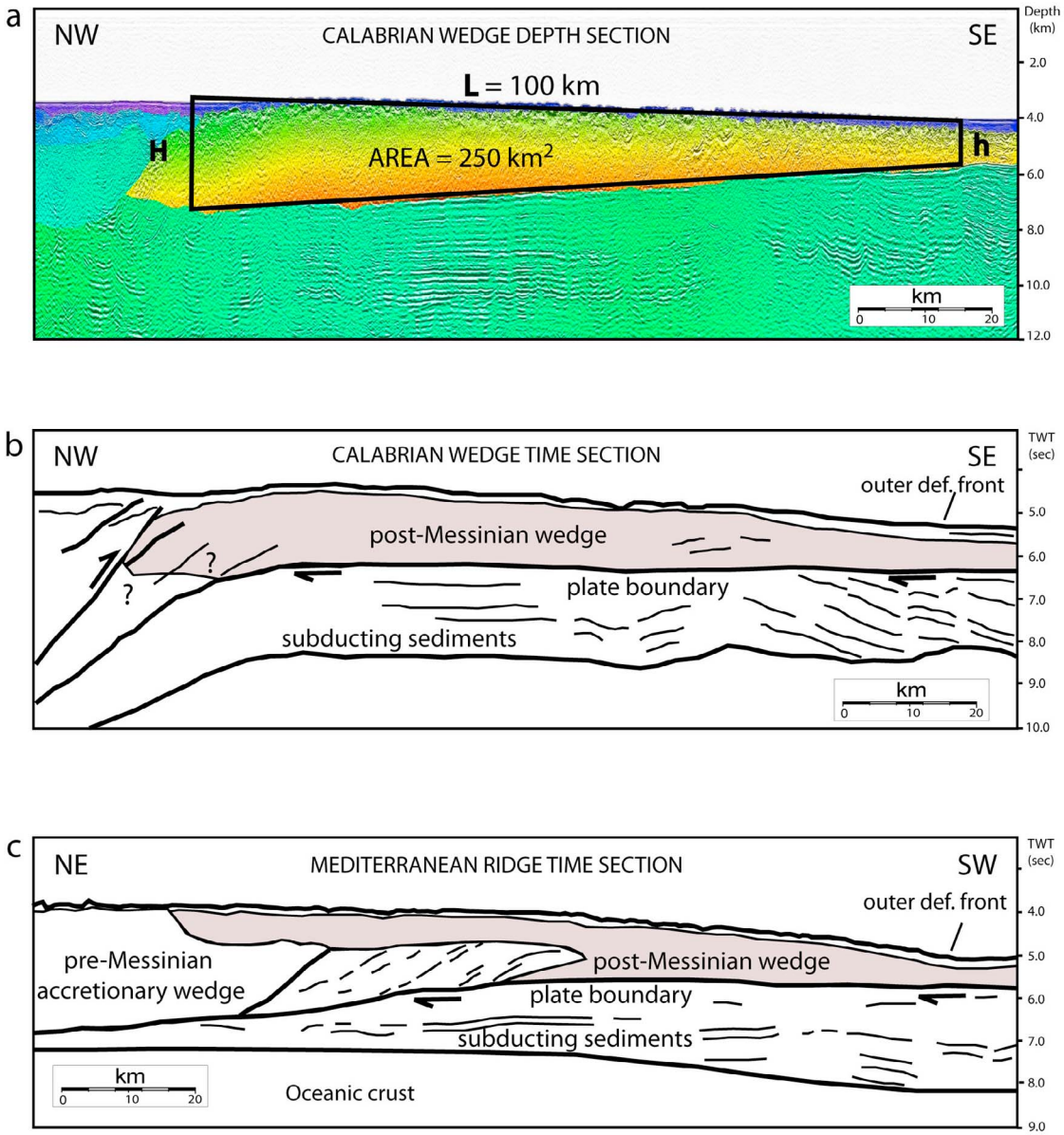

Figure 16. (a) Pre-stack depth migrated MCS line CROP M-2B with color-code seismic velocities derived from seismic data migration. Location of seismic profile is shown in Figure 2. (b) Simplified line drawing of the time migrated seismic line CROP M-2B. The post-Messinian wedge has been highlighted with a gray pattern. (c) Simplified line drawing of a time migrated seismic section across the Mediterranean Ridge (modified from *Reston et al.* [2002]). The two accretionary wedges have similar size despite the Mediterranean Ridge is growing ten times faster than the Calabrian Arc.

agreement with *Mattei et al.* [2007] who suggested that vertical axis rotations in the CA ceased in the uppermost part of the Lower Pleistocene (about 1 Ma ago); this is interpreted as a decreased efficiency of the tectonic processes related to the Ionian slab that caused on one hand a halting of the back-arc opening in the Southern Tyrrhenian Sea and on the other the decrease in convergence rate along the Ionian trench;

[65] 2. Sediment thickness in the abyssal plain during the last 4–5 Ma might be larger. This is unlikely because the thickness of the evaporites is rather constant in the central Mediterranean Sea.

[66] 3. Wedge building process is independent on convergence rate.

[67] According to (1), and assuming that during the last 5 Ma the entire sedimentary section above the basal detachment has been frontally accreted, we can derive a long-term convergence rate of 3.7 cm/yr. This value is very high if compared to the present-day GPS estimated rate, but comparable to the slab retreat velocity for the last 5 Ma proposed by *Gueguen et al.* [1998]. Trench migration during the last 40 Myr as reconstructed by *Faccenna et al.* [2001] is not linear but rather related to a succession of tectonic phases linked to the opening and extension in the Tyrrhenian

basin. From 15 to 10 Ma a decrease in subduction velocity (1–2 cm/yr) is related to a slow trench roll back before the onset of the main phases of Tyrrhenian extension. Afterwards, between 5 and 3 Ma, subduction velocity increased producing a fast outer wedge growth while recently trench roll back has slowed again [*Minelli and Faccenna*, 2010]. The size of the outer accretionary wedge as reconstructed through our work is the result of this nonlinear trench retreat averaged over 5 Ma.

[68] Thermal modeling of the Calabrian subduction provides elements to constrain long-term subduction velocities [*Gutscher et al.*, 2006]. Indeed, the high heat flow (150–200 mW/m^2) observed in the SE Tyrrhenian basin indicates vigorous mantle convection below. High subduction velocity (1 cm/yr or more) supplied to numerical models led to a better agreement between observed and predicted heat flow [*Gutscher et al.*, 2006]. However, these relatively high velocities represent an average over the past few million years, and may not be indicative of the present-day regime.

[69] To better understand the apparent discrepancy between the convergence rate and the amount of accreted sediments during the last 5 Ma, we have compared the size and geometry of the CA accretionary wedge to the Mediterranean Ridge. The Mediterranean Ridge accretionary history is similar to that of the CA because it is a salt bearing accretionary wedge emplaced in two distinct phases separated by the deposition of the Messinian evaporites [*Chaumillon and Mascle*, 1997] that has strongly affected the structural style and the wedge building. Figure 16b shows a line drawing of the time section of MCS line CROP M-2B across the western CA while Figure 16c is a schematic line drawing of the Mediterranean Ridge after *Reston et al.* [2002]. The two wedges have comparable width and thickness; thus the volume per unit section of accreted material during post-Messinian times is roughly the same despite the very different convergence rates. This comparison suggests that wedge growth may be nonlinear and/or independent on convergence velocity, as proposed for the Barbados wedge by *Le Pichon et al.* [1990]. In this reconstruction variations in the rate of slab roll-back and/or the dramatic Messinian salinity crisis play a fundamental role in driving wedge building processes.

6. Conclusion

[70] We used an integrated interpretation of a multiscale seismic reflection data set to describe the tectonic setting of the Calabrian Arc, along the African-Eurasian plate boundary in the Ionian Sea. Several tectonic domains were described, and a kinematic reconstruction based on structural and stratigraphic constraints provided by the analysis of depth-migrated crustal sections. High resolution multi and single-channel seismic reflection profiles were used to map active, potentially seismogenic features that could have caused the historical destructive earthquakes of the region. We found the following.

[71] 1. The emplacement of the Messinian evaporites in the sedimentary section produced an abrupt change in wedge building processes marked by variations in topographic slope angles, basal detachment depths, as well as variations in structural style and deformation rates. The very low tapered post-Messinian accretionary wedge in the western region of the CA is a salt bearing accretionary complex where frontal accretion of the Messinian and Plio-Quaternary units do actually occur along a basal detachment located at the base of the Messinian evaporites. The pre-Messinian accretionary wedge is constituted by Tertiary and Mesozoic sediments; here the basal detachment is located at the top of the Mesozoic carbonates or oceanic basement. Underplating processes and duplex formation are active in this region. The transition between the post and pre- Messinian accretionary wedges is the locus of complex faulting that enhances fluid flow and mud diapirism.

[72] 2. The CA subduction complex is segmented longitudinally into two different lobes delimited by a NW/SE deformation zone that accommodates differential movements of the Calabrian and the Peloritan portions of CA. This can explain the NW-SE extension observed in the straits of Messina as well as why Calabria has advanced further SE relative to NE Sicily. The formation of the two lobes and their evolution may be driven by additional factors, such as tectonic rotations related to different rates of collision with the Mediterranean Ridge along the irregular Africa/Eurasia plate boundary and generally by plate fragmentation during the terminal stages of subduction. Structural style variations, such as taper angles, uplift rates and seafloor morphologies within the two lobes, suggest different rates of plate coupling on the subduction thrust with those in the Eastern lobe facing Calabria being higher. We propose these two lobes represent two distinct domains of the subduction complex, characterized by different stages of subduction and/or plate fragmentation in the Ionian Sea. In particular, the WL corresponds to areas where the slab is already detached, while the EL corresponds to the region of the CA where local earthquake tomographic maps image a in depth continuous slab penetrating into the mantle.

[73] 3. The post-Messinian CA subduction complex has structural style, width and geometries similar to the recent Western Mediterranean Ridge, suggesting it is growing at a similar rate despite the very different convergence velocities reported by GPS data. Simple cross-sectional area balancing made on the depth seismic section imply that the CA long-term subduction velocity, averaged over the last 5 Ma, is in the order of 3.5 cm/yr, about 10 times higher than GPS current motion. This suggests that convergence rate has slowed down significantly in recent times (1 Ma) or that the outward wedge velocity changed through time, being much faster than the subduction rate during the emplacement of the evaporites. The Messinian times may thus be seen as a new cycle in the accretion, possibly characterized by high growth rates of the accretionary wedge.

[74] 4. Seismic data reveal the existence of both compressive and transtensive active faults in the subduction complex. We propose a lithospheric NW/SE trending transtensive fault at about 70 km E of the toe of the Malta escarpment as the shallow expression of a STEP fault. In our interpretation, this structure, together with the boundary between the two lobes and a set of out-of-sequence thrust faults (SPLAYS) at the transition between the pre- and post-Messinian wedges, represents seismogenic features likely to have generated major earthquakes in the past. In fact, these structures are active, are large (100 km), are deeply rooted, and bounds sectors of the margin characterized by different deformation rates. In particular, the

observed out-of-sequence thrust faults reflect the structural contrast between a shallow décollement (Messinian evaporites) in the frontal wedge and a deeper basal detachment within the pre-Messinian sediments, primarily due to differences in rheology. The out-of-sequence thrust faults in the Eastern lobe (offshore Calabria) should be taken into account for any reliable seismic risk assessment because this subduction lobe is characterized by higher deformation rates and steeper structures in depth.

[75] Finally, we suggest that the proposed lithospheric structure between the two lobes of the CA plays a fundamental role in controlling subduction processes and margin segmentation. The lack of thrust-type seismicity along the CA complex may indicate that subduction is active but aseismic or that plate motion is expressed by large earthquakes with long recurrence time intervals. If subduction has stopped recently the prism is deforming not by underthrusting of an oceanic plate but, rather, by a more distributed deformation related to the still ongoing plate convergence. In this latter case, the proposed structure between the EL and WL may represent a recent boundary in a overall plate re-organization tectonic phase.

[76] The segmented geometry of the CA subduction complex, the very old African subducting oceanic crust and the slow convergence rates should, however, prevent the occurrence of earthquakes with M > 7.5.

[77] **Acknowledgments.** The CALAMARE scientific party (G. Bortoluzzi, C. Carmisciano, G. Carrara, M. Cuffaro, F. D'Oriano, M. Gambetta, M. Ligi, X. Locritani, L. Minelli, F. Muccino, D. Oppo, and I. Viola), Captain Lubrano, and the Urania shipboard and SOPROMAR parties are greatly acknowledged for their important contribution in data acquisition during the Urania cruise. We greatly acknowledge the CIESM/Ifremer Medimap group [*Loubrieu et al.*, 2008] for having provided us with the multibeam grid of the study area. Most maps were generated using the GMT software [*Wessel and Smith*, 1991], while structural mapping was performed with the SeisPrho software [*Gasperini and Stanghellini*, 2009]. We thank Enrico Bonatti, Claudio Faccenna, Salvatore Barba, and Carlo Doglioni for useful discussions. This work has been supported by MIUR-PRIN, 2006 (L. Torelli and R. Capozzi) and TOPOMED projects and has benefited from funding provided by the Italian Presidenza del Consiglio dei Ministri - Dipartimento della Protezione Civile (DPC). We acknowledge the Editor, Onno Oncken; Cesar Ranero; and two anonymous reviewers for their suggestions and comments that have contributed to the improvement of the original version of the manuscript. One special thought is addressed to Davide, for all he shared and transmitted to the first author and L. Gasperini during his very short life. This is ISMAR paper 1718.

References

Argnani, A., and C. Bonazzi (2005), Malta Escarpment fault zone offshore eastern Sicily: Plio-Quaternary tectonic evolution based on new multichannel seismic data, *Tectonics*, *24*, TC4009, doi:10.1029/2004TC001656.

Bigi, S., F. Lenci, C. Doglioni, J. C. Moore, E. Carminati, and D. Scrocca (2003), Décollement depth versus accretionary prism dimension in the Apennines and the Barbados, *Tectonics*, *22*(2), 1010, doi:10.1029/2002TC001410.

Billi, A., G. Barberi, C. Faccenna, G. Neri, F. Pepe, and A. Sulli (2006), Tectonics and seismicity of the Tindari Fault System, southern Italy: Crustal deformation at the transition between ongoing contractional and extensional domains located above the edge of a subducting slab, *Tectonics*, *25*, TC2006, doi:10.1029/2004TC001763.

Billi, A., D. Presti, C. Faccenna, N. Neri, and B. Orecchio (2007), Seismotectonics of the Nubia plate compressive margin in the south Tyrrhenian region, Italy: Clues for subduction inception, *J. Geophys. Res.*, *112*, B08302, doi:10.1029/2006JB004837.

Bonardi, G., W. Cavazza, V. Peruarone, and S. Rossi (2001), Calabria-Peloritani terrane and northern Ionian Sea, in *Anatomy of an Orogen: The Apennines and Adjacent Mediterranean Basins*, edited by G. B. Vai and I. P. Martini, pp. 286–306, Kluwer Acad., Dordrecht, Netherlands.

Bottari, A., P. Capuano, G. De Natale, P. Gasparini, G. Neri, F. Pingue, and R. Scarpa (1989), Source parameters of earthquakes in the Strait of Messina, Italy, during this century, *Tectonophysics*, *166*, 221–234, doi:10.1016/0040-1951(89)90215-1.

Calais, E., C. DeMets, and J. M. Nocquet (2003), Evidence for a post-3.16 Ma change in Nubia–Eurasia–North America plate motions?, *Earth Planet. Sci. Lett.*, *216*, 81–92, doi:10.1016/S0012-821X(03)00482-5.

Camerlenghi, A., and M. B. Cita (1987), Setting and tectonic evolution of some eastern Mediterranean deep-sea basins, *Mar. Chem.*, *75*, 31–56, doi:10.1016/0025-3227(87)90095-8.

Catalano, R., C. Doglioni, and S. Merlini (2001), On the Mesozoic Ionian Basin, *Geophys. J. Int.*, *144*, 49–64, doi:10.1046/j.0956-540X.2000.01287.x.

Cernobori, L., A. Hirn, J. H. McBride, R. Nicolich, L. Petronio, M. Romanelli, and Streamers/Profiles Working Groups (1996), Crustal image of the Ionian basin and its Calabrian margins, *Tectonophysics*, *264*, 175–189, doi:10.1016/S0040-1951(96)00125-4.

Chamot-Rooke, N., A. Rabaute, and C. Kreemer (2005a), Western Mediterranean Ridge mud belt correlates with active shear strain at the prism-backstop geological contact, *Geology*, *33*, 861–864, doi:10.1130/G21469.1.

Chamot-Rooke, N., C. Rangin, X. Le Pichon, and DOTMED Working Group (2005b), DOTMED–Deep Offshore Tectonics of the Mediterranean: A synthesis of deep marine data in eastern Mediterranean [CD-ROM], *Mem. Soc. Geol. Fr.*, *177*, 64 pp.

Chaumillon, E., and J. Mascle (1997), From foreland to forearc domains: New multichannel seismic reflection survey of the Mediterranean Ridge accretionary complex (eastern Mediterranean), *Mar. Geol.*, *138*, 237–259, doi:10.1016/S0025-3227(97)00002-9.

Chaumillon, E., J. Mascle, and H. J. Hoffmann (1996), Deformation of the western Mediterranean Ridge: Importance of Messinian evaporitic formations, *Tectonophysics*, *263*, 163–190, doi:10.1016/S0040-1951(96)00035-2.

Chiarabba, C., L. Jovane, and R. DiStefano (2005), A new view of Italian seismicity using 20 years of instrumental recording, *Tectonophysics*, *395*, 251–268, doi:10.1016/j.tecto.2004.09.013.

Cummins, P. R., and Y. Kaneda (2000), Possible splay fault slip during the 1946 Nankai earthquake, *Geophys. Res. Lett.*, *27*, 2725–2728, doi:10.1029/1999GL011139.

D'Agostino, N., and G. Selvaggi (2004), Crustal motion along the Eurasia-Nubia plate boundary in the Calabrian Arc and Sicily and active extension in the Messina Straits from GPS measurements, *J. Geophys. Res.*, *109*, B11402, doi:10.1029/2004JB002998.

D'Agostino, N., A. Avallone, D. Cheloni, E. D'Anastasio, S. Mantenuto, and G. Selvaggi (2008), Active tectonics of the Adriatic region from GPS and earthquake slip vectors, *J. Geophys. Res.*, *113*, B12413, doi:10.1029/2008JB005860.

de Voogd, B., C. Truffert, N. Chamot-Rooke, P. Huchon, S. Lallemant, and X. Le Pichon (1992), Two-ship deep seismic soundings in the basins of the eastern Mediterranean Sea (Pasiphae cruise), *Geophys. J. Int.*, *109*, 536–552, doi:10.1111/j.1365-246X.1992.tb00116.x.

DeCelles, P. G., and W. Cavazza (1995), Upper Messinian conglomerates in Calabria, southern Italy: Response to orogenic wedge adjustment following Mediterranean sea-level changes, *Geology*, *23*(9), 775–778, doi:10.1130/0091-7613(1995)023<0775:UMCICS>2.3.CO;2.

Del Ben, A., C. Barnaba, and A. Taboga (2008), Strike-slip systems as the main tectonic features in the Plio-Quaternary kinematics of the Calabrian Arc, *Mar. Geophys. Res.*, *29*, 1–12, doi:10.1007/s11001-007-9041-6.

Devoti, R., F. Riguzzi, M. Cuffaro, and C. Doglioni (2008), New GPS constraints on the kinematics of the Apennines subduction, *Earth Planet. Sci. Lett.*, *273*, 163–174, doi:10.1016/j.epsl.2008.06.031.

Doglioni, C., S. Merlini, and G. Cantarella (1999), Foredeep geometries at the front of the Apennines in the Ionian Sea (central Mediterranean), *Earth Planet. Sci. Lett.*, *168*, 243–254, doi:10.1016/S0012-821X(99)00059-X.

Doglioni, C., F. Innocenti, and G. Mariotti (2001), Why Mt Etna?, *Terra Nova*, *13*(1), 25–31, doi:10.1046/j.1365-3121.2001.00301.x.

Doglioni, C., E. Carminati, and M. Cuffaro (2006), Simple kinematics of subduction zones, *Int. Geol. Rev.*, *48*, 479–493, doi:10.2747/0020-6814.48.6.479.

Doglioni, C., E. Carminati, M. Cuffaro, and D. Scrocca (2007), Subduction kinematics and dynamic constraints, *Earth Sci. Rev.*, *83*, 125–175, doi:10.1016/j.earscirev.2007.04.001.

Faccenna, C., T. W. Becker, F. P. Lucente, L. Jolivet, and F. Rossetti (2001), History of subduction and back-arc extension in the central Mediterranean, *Geophys. J. Int.*, *145*, 809–820, doi:10.1046/j.0956-540x.2001.01435.x.

Faccenna, C., C. Piromallo, A. Crespo-Blanc, L. Jolivet, and F. Rossetti (2004), Lateral slab deformation and the origin of the western Mediterranean arcs, *Tectonics*, *23*, TC1012, doi:10.1029/2002TC001488.

Finetti, I. (1976), Mediterranean Ridge: A young submerged chain associated with the Hellenic Arc, *Boll. Geofis. Teor. Appl.*, *13*, 31–65.

Finetti, I. (1982), Structure, stratigraphy, and evolution of central Mediterranean, *Boll. Geofis. Teor. Appl.*, *24*, 247–312.

Finetti, I. (2005), *CROP Project: Deep Seismic Exploration of the Central Mediterranean and Italy*, *Atlases Geosci.*, vol. 1, Elsevier, Amsterdam.

Frepoli, A., G. Selvaggi, C. Chiarabba, and A. Amato (1996), State of stress in the southern Tyrrhenian subduction zone from fault-plane solutions, *Geophys. J. Int.*, *125*, 879–891, doi:10.1111/j.1365-246X.1996.tb06031.x.

Fuller, C. W., S. D. Willett, and M. T. Brandon (2006), Formation of forearc basins and their influence on subduction zone earthquakes, *Geology*, *34*, 65–68, doi:10.1130/G21828.1.

Galli, P., and V. Bosi (2003), Catastrophic 1638 earthquakes in Calabria (southern Italy): New insights from paleoseismological investigation, *J. Geophys. Res.*, *108*(B1), 2004, doi:10.1029/2001JB001713.

Gasperini, L., and G. Stanghellini (2009), SeisPrho: An interactive computer program for processing and interpretation of high-resolution seismic reflection profiles, *Comput. Geosci.*, *35*, 1497–1507, doi:10.1016/j.cageo.2008.04.014.

Goes, S., D. Giardini, S. Jenny, C. Hollenstein, H.-G. Kahle, and A. Geiger (2004), A recent tectonic reorganization in the south-central Mediterranean, *Earth Planet. Sci. Lett.*, *226*, 335–345, doi:10.1016/j.epsl.2004.07.038.

Govers, R., and M. J. R. Wortel (2005), Lithosphere tearing at STEP faults: Response to edges of subduction zones, *Earth Planet. Sci. Lett.*, *236*, 505–523, doi:10.1016/j.epsl.2005.03.022.

Gueguen, E., C. Doglioni, and M. Fernandez (1998), On the post-25 Ma geodynamic evolution of the western Mediterranean, *Tectonophysics*, *298*, 259–269, doi:10.1016/S0040-1951(98)00189-9.

Guillaume, B., F. Funiciello, C. Faccenna, J. Martinod, and V. Olivetti (2010), Spreading pulses of the Tyrrhenian Sea during the narrowing of the Calabrian slab, *Geology*, *38*, 819–822, doi:10.1130/G31038.1.

Gutscher, M.-A., J. Roger, M.-A. Baptista, J. M. Miranda, and S. Tinti (2006), Source of the 1693 Catania earthquake and tsunami (southern Italy): New evidence from tsunami modeling of a locked subduction fault plane, *Geophys. Res. Lett.*, *33*, L08309, doi:10.1029/2005GL025442.

Gvirtzman, Z., and A. Nur (2001), Residual topography, lithospheric structure and sunken slabs in the central Mediterranean, *Earth Planet. Sci. Lett.*, *187*, 117–130, doi:10.1016/S0012-821X(01)00272-2.

Hersey, J. B. (1965), Sedimentary basins of the Mediterranean Sea, in *Submarine Geology and Geophysics: Proceedings of the 17th Symposium, Held in the University of Bristol, 5–9 April*, edited by W. F. Whitard and W. Bradshaw, pp. 75–91, Butterworths, London.

Hinz, K. (1972), Zum Diapirismus im westlichen Mittelmeer, *Geol. Jahrb.*, *90*, 389–396.

Hollenstein, C., H.-G. Kahle, A. Geiger, S. Jenny, S. Goes, and D. Giardini (2003), New GPS constraints on the Africa-Eurasia plate boundary zone in southern Italy, *Geophys. Res. Lett.*, *30*(18), 1935, doi:10.1029/2003GL017554.

Jacques, E., C. Monaco, P. Tapponnier, L. Tortorici, and T. Winter (2001), Faulting and earthquake triggering during the 1783 Calabria seismic sequence, *Geophys. J. Int.*, *147*, 499–516, doi:10.1046/j.0956-540x.2001.01518.x.

Jenny, S., S. Goes, D. Giardini, and H.-G. Kahle (2006), Seismic potential of southern Italy, *Tectonophysics*, *415*, 81–101, doi:10.1016/j.tecto.2005.12.003.

Jolivet, L., and C. Faccenna (2000), Mediterranean extension and the Africa-Eurasia collision, *Tectonics*, *19*, 1095–1106, doi:10.1029/2000TC900018.

Kastens, K. A. (1981), Structural causes and sedimentological effects of "cobblestone" topography in the eastern Mediterranean Sea, Ph.D. thesis, Scripps Inst. of Oceanogr., La Jolla, Calif.

Kastens, K. A. (1991), Rate of outward growth of the Mediterranean Ridge accretionary complex, *Tectonophysics*, *199*, 25–50, doi:10.1016/0040-1951(91)90117-B.

Kastens, K. A., and M. B. Cita (1981), Tsunami-induced sediment transport in the abyssal Mediterranean Sea, *Geol. Soc. Am. Bull.*, *92*, 845–857, doi:10.1130/0016-7606(1981)92<845:TSTITA>2.0.CO;2.

Kimura, G., G. F. Moore, M. Strasser, E. Screaton, D. Curewitz, C. Streiff, and H. Tobin (2011), Spatial and temporal evolution of the megasplay fault in the Nankai Trough, *Geochem. Geophys. Geosyst.*, *12*, Q0A008, doi:10.1029/2010GC003335.

Lallemand, S. E., P. Schnürle, and J. Malavieille (1994), Coulomb theory applied to accretionary and nonaccretionary wedges: Possible causes for tectonic erosion and/or frontal accretion, *J. Geophys. Res.*, *99*, 12,033–12,055, doi:10.1029/94JB00124.

Le Pichon, X., P. Henry, and S. Lallemant (1990), Water flow in the Barbados accretionary complex, *J. Geophys. Res.*, *95*, 8945–8967, doi:10.1029/JB095iB06p08945.

Loubrieu, B., et al. (2008), Morpho-bathymetry of the Mediterranean Sea, special publication, Int. Comm. for Sci. Explor. of the Mediterr. Sea, Monaco.

Lucente, F. P., L. Margheriti, C. Piromallo, and G. Barruol (2006), Seismic anisotropy reveals the long route of the slab through the western-central Mediterranean mantle, *Earth Planet. Sci. Lett.*, *241*, 517–529, doi:10.1016/j.epsl.2005.10.041.

MacKay, S., and R. Abma (1993), Depth-focusing analysis using a wavefront-curvature criterion, *Geophysics*, *58*, 1148–1156, doi:10.1190/1.1443498.

Makris, J., R. Nicolich, and W. Weigel (1986), A seismic study in the western Ionian Sea, *Ann. Geophys., Ser. B*, *6*, 665–678.

Malinverno, A., and W. B. F. Ryan (1986), Extension in the Tyrrhenian Sea and shortening in the Apennines as result of arc migration driven by sinking of the lithosphere, *Tectonics*, *5*, 227–245, doi:10.1029/TC005i002p00227.

Marani, M. P., and T. Trua (2002), Thermal constriction and slab tearing at the origin of a superinflated spreading ridge: Marsili volcano (Tyrrhenian Sea), *J. Geophys. Res.*, *107*(B9), 2188, doi:10.1029/2001JB000285.

Mascle, J., and E. Chaumillon (1998), An overview of Mediterranean Ridge collisional accretionary complex as deduced from multichannel seismic data, *Geo Mar. Lett.*, *18*, 81–89, doi:10.1007/s003670050056.

Mattei, M., P. Cipollari, D. Cosentino, A. Argentieri, F. Rossetti, F. Speranza, and L. Di Bella (2002), The Miocene tectono-sedimentary evolution of the southern Tyrrhenian Sea: Stratigraphy, structural and paleomagnetic data from the on-shore Amantea basin (Calabrian Arc, Italy), *Basin Res.*, *14*, 147–168, doi:10.1046/j.1365-2117.2002.00173.x.

Mattei, M., F. Cifelli, and N. D'Agostino (2007), The evolution of the Calabrian Arc: Evidence from paleomagnetic and GPS observations, *Earth Planet. Sci. Lett.*, *263*, 259–274, doi:10.1016/j.epsl.2007.08.034.

Minelli, L., and C. Faccenna (2010), Evolution of the Calabrian accretionary wedge (central Mediterranean), *Tectonics*, *29*, TC4004, doi:10.1029/2009TC002562.

Montadert, L., J. Letouzey, and A. Mauffret (1978), Messinian event: Seismic evidence, *Initial Rep. Deep Sea Drill. Proj.*, *42*, 1021–1040, doi:10.2973/dsdp.proc.42-1.154.1978.

Morelli, A., et al. (2004), Geodynamic maps of the Mediterranean—Sheet 2: Seismicity and tectonics, 1:13,000,000 scale, Comm. for the Geol. Maps of the World, Paris.

Neri, G., B. Orecchio, C. Totaro, G. Falcone, and D. Presti (2009), Subduction beneath southern Italy close the ending: Results from seismic tomography, *Seismol. Res. Lett.*, *80*, 63–70, doi:10.1785/gssrl.80.1.63.

Park, J.-O., T. Tsuru, S. Kodaira, P. R. Cummins, and Y. Kaneda (2002), Splay fault branching along the Nankai subduction zone, *Science*, *297*, 1157–1160, doi:10.1126/science.1074111.

Pasquale, V., M. Verdoya, and P. Chiozzi (2005), Thermal structure of the Ionian slab, *Pure Appl. Geophys.*, *162*, 967–986, doi:10.1007/s00024-004-2651-x.

Patacca, E., and P. Scandone (2004), The Plio-Pleistocene thrust belt-foredeep system in the southern Apennines and Sicily (Italy), in *Geology of Italy: Special Volume of the Italian Geological Society for the IGC 32 Florence 2004*, edited by S. Crescenti et al., pp. 93–129, Soc. Geol. It., Rome.

Patacca, E., R. Sartori, and P. Scandone (1990), Tyrrhenian basin and Apenninic arcs: Kinematic relation since Late Tortonian times, *Mem. Soc. Geol. Ital.*, *45*, 425–451.

Piatanesi, A., and S. Tinti (1998), A revision of the 1693 eastern Sicily earthquake and tsunami, *J. Geophys. Res.*, *103*, 2749–2758, doi:10.1029/97JB03403.

Polonia, A., A. Camerlenghi, F. Davey, and F. Storti (2002), Accretion, structural style, and syn-contractional sedimentation in the eastern Mediterranean Sea, *Mar. Geol.*, *186*, 127–144, doi:10.1016/S0025-3227(02)00176-7.

Pondrelli, S., C. Piromallo, and E. Serpelloni (2004), Convergence vs. retreat in southern Tyrrhenian Sea: Insights from kinematics, *Geophys. Res. Lett.*, *31*, L06611, doi:10.1029/2003GL019223.

Praeg, D., S. Ceramicola, R. Barbieri, V. Unnithan, and N. Wardell (2009), Tectonically-driven mud volcanism since the late Pliocene on the Calabrian accretionary prism, central Mediterranean Sea, *Mar. Pet. Geol.*, *26*, 1849–1865, doi:10.1016/j.marpetgeo.2009.03.008.

Reilinger, R., et al. (2006), GPS constraints on continental deformation in the Africa-Arabia-Eurasia continental collision zone and implications for the dynamics of plate interactions, *J. Geophys. Res.*, *111*, B05411, doi:10.1029/2005JB004051.

Reston, T. J., R. von Huene, T. Dickmann, D. Klaeschen, and H. Kopp (2002), Frontal accretion along the western Mediterranean Ridge: The

effect of the Messinian evaporites on wedge mechanics and structural style, *Mar. Geol.*, *186*, 59–82, doi:10.1016/S0025-3227(02)00173-1.

Rossetti, F., B. Goffe, P. Monie, C. Faccenna, and G. Vignaroli (2004), Alpine orogenic P-T-t deformation history of the Catena Costiera area and surrounding regions (Calabrian Arc, southern Italy): The nappe edifice of north Calabria revised with insights on the Tyrrhenian-Apennine system formation, *Tectonics*, *23*, TC6011, doi:10.1029/2003TC001560.

Rossi, S., and R. Sartori (1981), A seismic reflection study of the external Calabrian arc in the northern Ionian Sea (eastern Mediterranean), *Mar. Geophys. Res.*, *4*, 403–426, doi:10.1007/BF00286036.

Ryan, W. B. F., et al. (Eds.) (1973), *Initial Reports of the Deep Sea Drilling Project*, *Leg 13*, vol. 13, 1447 pp., U.S. Gov. Print. Off., Washington, D. C., doi:10.2973/dsdp.proc.13.1973.

Sartori, R. (2003), The Tyrrhenian back-arc basin and subduction of the Ionian lithoshere, *Episodes*, *26*, 217–221.

Satake, K., K. L. Wang, and B. F. Atwater (2003), Fault slip and seismic moment of the 1700 Cascadia earthquake inferred from Japanese tsunami descriptions, *J. Geophys. Res.*, *108*(B11), 2535, doi:10.1029/2003JB002521.

Selvaggi, G., and C. Chiarabba (1995), Seismicity and P-wave velocity image of the southern Tyrrhenian subduction zone, *Geophys. J. Int.*, *121*, 818–826, doi:10.1111/j.1365-246X.1995.tb06441.x.

Serpelloni, E., G. Vannucci, S. Pondrelli, A. Argnani, G. Casula, M. Anzidei, P. Baldi, and P. Gasperini (2007), Kinematics of the western Africa-Eurasia plate boundary from focal mechanisms and GPS data, *Geophys. J. Int.*, *169*, 1180–1200, doi:10.1111/j.1365-246X.2007.03367.x.

Sibuet, J. C., et al. (2007), 26 December 2004 great Sumatra-Andaman earthquake: Co-seismic and post-seismic motions in northern Sumatra, *Earth Planet. Sci. Lett.*, *263*, 88–103, doi:10.1016/j.epsl.2007.09.005.

Wells, R. E., R. J. Blakely, Y. Sugiyama, D. S. Scholl, and A. Dinterman (2003), Basin-centered asperities in great subduction zone earthquakes: A link between slip, subsidence, and subduction erosion?, *J. Geophys. Res.*, *108*(B10), 2507, doi:10.1029/2002JB002072.

Wessel, P., and W. H. F. Smith (1991), Free software helps map and display data, *Eos Trans. AGU*, *72*, 441, doi:10.1029/90EO00319.

Westaway, R. (1993), Quaternary uplift of southern Italy, *J. Geophys. Res.*, *98*, 21,741–21,772, doi:10.1029/93JB01566.

Wortel, M. J. R., and W. Spakman (2000), Subduction and slab detachment in the Mediterranean-Carpathian region, *Science*, *290*, 1910–1917, doi:10.1126/science.290.5498.1910.

Zito, G., F. Mongelli, S. De Lorenzo, and C. Doglioni (2003), Heat flow and geodynamics in the Tyrrhenian Sea, *Terra Nova*, *15*, 425–432, doi:10.1046/j.1365-3121.2003.00507.x.

A. Artoni, P. Mussoni, and L. Torelli, Dipartimento di Scienze della Terra, University of Parma, Parco Area delle Scienze 157/A, I-43100 Parma, Italy. (andrea.artoni@unipr.it; paola.mussoni@unipr.it; lutor@unipr.it)

L. Gasperini and A. Polonia, Institute of Marine Sciences, ISMAR-Bo, CNR, Via Gobetti 101, I-40129 Bologna, Italy. (luca.gasperini@ismar.cnr.it; alina.polonia@ismar.cnr.it)

D. Klaeschen, Leibniz-Institut für Meereswissenschaften (IFM-GEOMAR), Wischhofstr. 1-3, D-24148 Kiel, Germany. (dklaeschen@ifm-geomar.de)